TECHNICAL INFORMATION SERIES

MECHANICS OF COMPOSITE STRENGTHENING

SPACE SCIENCES
LABORATORY

MISSILE AND SPACE DIVISION
GENERAL ELECTRIC

SPACE SCIENCES LABORATORY

MECHANICS SECTION

MECHANICS OF COMPOSITE STRENGTHENING*

By

B. Walter Rosen

*Presented at the ASM Seminar on Fiber Composite Materials, October 17, 1964, Philadelphia, Pa.

R64SD80
November 1964

MISSILE AND SPACE DIVISION

GENERAL ELECTRIC

MECHANICS OF COMPOSITE STRENGTHENING*

by B. Walter Rosen

ABSTRACT

The development of very high strength and stiffness filaments has motivated considerable interest in the strength of fiber reinforced composites. The purpose of the present paper is to describe studies of the effect of fiber and matrix characteristics upon the mechanics of deformation and fracture of fibrous composites. These studies consider the response of a matrix reinforced by uniaxially oriented fibers. The strength of such a material is treated for the cases where the failure criteria are maximum tensile of compressive load carried by the composite in a direction parallel to the fiber orientation. Analytical models for failure in these two modes are developed. Comparison is made with available experimental data. The tensile failure model is a statistical one. A new experimental technique to investigate the validity of this model is described. All of the studies included attempt to relate composite performance to constituent properties.

* This research was supported by the National Aeronautics and Space Administration under contract NASw-817.

TABLE OF CONTENTS

SUMMARY

The existence of many very high strength and stiffness filaments has motivated considerable interest in the selection of appropriate matrix materials to obtain fibrous composites which can utilize these outstanding properties. It is the purpose of the present paper to describe studies of the influence of both fiber and matrix characteristics upon the mechanics of deformation and fracture of fibrous composites. The aim is to obtain the information needed to select appropriate constituents for given applications. These studies consider the response of a matrix reinforced by uniaxially oriented fibers. The strength of such a material is treated for the cases where the failure criteria are maximum tensile and compressive loads carried by the composite in a direction parallel to the fiber orientation.

When the response of a composite is to be measured in terms of average stress and average strain, the material can be represented by an effective homogeneous but anisotropic material having the same average response. For the case of a matrix containing uniaxially oriented fibers, the effective material is transversely isotropic and is therefore characterized by five elastic constants. Various analytical approaches to the evaluation of these constants as functions of the constituent properties have been made and the relationship between constituent properties and elastic moduli is reasonably well understood.

However, when a fracture criterion is desired, an understanding of the average stress-strain response is no longer sufficient, and consideration must be given to internal irregularities in the state of stress. The present paper treats these problems for both ultimate compressive and tensile strengths.

The failure of a fibrous composite under a uniaxial compressive load is considered first. A possible failure mechanism for this case is the hypothesis that the individual fibers buckle in a short wave length pattern in a fashion analogous to the buckling of a column or plate on an elastic foundation. An approximate evaluation of the influence of fiber geometry and fiber and matrix moduli upon the composite compressive strength can then be made.

These results are compared to the results of an experimental program which utilized hollow and solid glass fibers in several matrix materials. The test specimens were short columns designed to achieve a compressive strength failure.

The major portion of the present paper is devoted to a study of the mechanics of tensile failure of a fibrous composite. The study is based upon consideration of the phenomena which occur subsequent to an initial internal fracture. The strength of the brittle fibers are considered to be defined by a statistical distribution function. Thus, the initial fracture is likely to occur in a fiber. The resulting perturbation of the local stress field is treated. An approximate solution indicates the nature of the interface stress distribution as well as stress concentrations in nearby fibers. This stress field could result in adjacent fiber fracture, that is a crack propagation effect; or in separation along the interface. A third possibility is that the stresses in the vicinity of an initial fiber fracture do not produce further fracture and that increasing load produces a distribution of fiber fractures corresponding to the initial distribution of weak points in the fibers. The continued accumulation of these fractures would produce a weak cross-section at which the remaining unbroken fibers could no longer transmit the applied load. Instantaneous tensile failure would then occur.

A statistical tensile failure model of a fibrous composite is established on this basis. The mechanical characteristics of fiber and matrix are utilized to obtain a statistical failure definition. An experimental program to investigate the validity of the model is described. The specimens are thin glass-reinforced epoxy specimens which are observed photoelastically during the loading process. An attempt is made to correlate the tensile properties of constituents and composites.

All of the studies included attempt to relate composite performance to constituent properties. In general, the constituents have been treated as homogeneous isotropic materials. The implications of the assumptions are treated in the comparison with experimental data.

TENSILE STRENGTH

The tensile failure of a uniaxially stiffened matrix has been studied previously by several investigators. The early findings are summarized in Ref. 1. The simplest failure model treated assumes that a uniform strain exists throughout the composite and that fracture occurs at the failure strain of the fibers alone (e.g. Ref. 2). The effect of a non-uniform strain distribution was studied in Ref. 3 which suggests the influence of fiber flaws on composite failure. In Ref. 3, failure occurs when the accumulation of fiber fractures resulting from increasing load shortens the fiber lengths to the point that further increases in load could not be transmitted to the fibers because the maximum matrix shear stress was exceeded. Thus, composite failure resulted from a shear failure of the matrix. There continues to be substantial disagreement as to the actual mechanics of failure within such a composite.

The model treated in the present analysis (see Ref. 4) is shown in Figure 1, and consists of a set of parallel fibers which are assumed to be strong and stiff with respect to the matrix material in which they are imbedded. The fibers treated are high strength brittle fibers whose strength is dependent upon the degree of surface imperfection. When such a composite is subjected to a tensile load a fiber fracture will occur at one of the serious flaws or imperfections. When such a fiber breaks, the stress in the vicinity of the broken fiber is perturbed substantially so that the axial stress in the fiber vanishes at the fiber break and gradually builds back up to its undisturbed stress value due to shear stresses being transferred across the fiber matrix interface. The general form of the local stress pattern in the fiber is shown in the figure. When such a break occurs, several possibilities for the future behavior of the composite exist. First, the high interface shear stresses could produce interface failure which could propagate along the length of the fiber reducing the fiber effectiveness over a substantial fiber length. In order to achieve the potential of the fiber strength it is necessary to study and determine the fabrication conditions which will yield an interface sufficiently strong to withstand this interface shear failure. This can be done either through the use of a high strength bond or a ductile matrix which

permits redistribution of the shear stresses. In the latter case the length of fiber which is affected by the break will increase as it will take a longer distance to retransmit the stresses back into the fiber at the low stress level of a ductile matrix. With a strong bond, the interface conditions can be overcome as a potential source of failure, and a second possibility is that the initial crack will propagate across the composite resulting in failure. This is influenced by the fracture toughness of the matrix and again since it is clear that with brittle fibers one can always expect a fracture to occur at a relatively low stress level, it is important that the fracture toughness of the matrix material be sufficient to prevent the propagation of this crack across the composite. If these two potential modes of failure are arrested it will then be possible to continue to increase the applied tensile load and to obtain breaks at other points of imperfection along the fibers. Increasing the load will produce a statistical accumulation of fiber fractures until a sufficient number of ineffective fiber lengths in the vicinity of one cross-section interact to provide a weak surface. At the point of incipient fracture all of the failure modes described may very well interact to produce the final fracture.

This statistical model of failure has been discussed in some detail in the previous work (Ref. 4). This portion of the present study is concerned with an extension of certain aspects of this problem to clarify the relationship between predicted results and experimental data, and to emphasize the potential for application of this analysis. A brief review of the method will be presented first.

The model which is used to evaluate the influence of constituent properties upon the tensile strength considers that in the vicinity of an individual break a portion of each fiber may be considered ineffective. The composite may then be considered to be composed of layers of dimension equal to the ineffective length. Any fiber which fractures within this layer will be unable to transmit a load across the layer. The applied load at that cross section would then be uniformly distributed among the unbroken fibers in each layer. The effect of stress concentrations which would introduce a non-uniform redistribution of these loads is not considered initially. A segment of a fiber within one of these layers may be considered as a link in the chain

which constitutes an individual fiber. Each layer of the composite is then a bundle of such links and the composite itself a series of such bundles. Treatment of a fiber as a chain of links is appropriate to the hypothesis that fracture is due to local imperfections. The links may be considered to have a statistical strength distribution which is equivalent to the statistical flaw distribution along the fibers. The realism of such a model is demonstrated by the length dependence of fiber strength. That is, longer chains have a high probability of having a weaker link than shorter chains, and this is supported by experimental data for brittle fibers which demonstrate that mean fiber strength is a monotonically decreasing function of fiber length. For this model it is first necessary to define a link dimension by consideration of the perturbed stress field in the vicinity of a broken fiber. It is then necessary to define the statistical strength distribution of the individual links which can be obtained indirectly from the experimental data for the fiber-strength-length relationship. These results can then be used in the statistical study of a series of bundles and utilized to define the distribution for the strength of the fibrous composite. (Statistical techniques for a series of bundles have been studied in Ref. 5 for application to particle reinforced composites.) The fibrous composite has been treated in Ref. 4 and portions of the following analysis are reproduced here from that reference for completeness.

Statistical Analysis of the Model

The model, as described in the previous section, consists of a chain of bundles of fiber links. The links have a length, δ, which is to be determined subsequently, and are characterized by a distribution function $f(\sigma)$ and the associated cumulative distribution function $F(\sigma)$, where:

$$F(\sigma) = \int_0^{\sigma} f(\sigma)\, d\sigma \tag{1}$$

and σ is the fiber stress. The experimental method for defining the distribution function will be described subsequently. With this distribution known, the distribution function for bundle strength can be obtained and then the composite will be treated as a chain of bundles, and weakest link statistical

theorems will be applied. This leads to the desired statistical definition of composite strength.

For a bundle of links, Daniels (Ref. 6) has shown that for a large number, N, of fibers the distribution of the average fiber stress at bundle failure, σ_B, approaches a normal distribution with expectation:

$$\bar{\sigma}_B = \sigma_m \left[1 - F(\sigma_m)\right] \tag{2}$$

and standard deviation:

$$\psi_B = \sigma_m \left\{F(\sigma_m)\left[1 - F(\sigma_m)\right]\right\}^{1/2} N^{-1/2} \tag{3}$$

The associated density distribution function is thus:

$$\omega(\sigma_B) = \frac{1}{\psi_B \sqrt{2\pi}} \exp\left[-1/2\left(\frac{\sigma_B - \bar{\sigma}_B}{\psi_B}\right)^2\right] \tag{4}$$

The maximum fiber stress, σ_m, is evaluated by maximizing the total load, which may be expressed as the product of the fiber stress and the number of unbroken fibers. Hence:

$$\frac{d}{d\sigma}\left\{\sigma\left[1 - F(\sigma)\right]\right\}_{\sigma = \sigma_m} = 0 \tag{5}$$

With the bundles characterized by eq. (4) and the associated cumulative distribution function, $\Omega(\sigma_B)$, given by:

$$\Omega(\sigma_B) = \int_0^{\bar{\sigma}_B} \omega(\sigma_B)\, d\sigma_B \tag{6}$$

The bundles may be treated as links in a chain and weakest link theorems can be applied to define composite failure. For m elements forming a chain

the distribution function, $\lambda(\sigma_c)$, for the average fiber stress at composite failure, σ_c, is defined by:

$$\lambda(\sigma_c = m\,\omega(\sigma_c))\left[1 - \Omega(\sigma_c)\right]^{m-1} \tag{7}$$

That is, $\lambda(\sigma_c)\,d\sigma_c$ is obtained by multiplying the probability that one bundle fails between σ_c and $\sigma_c + d\sigma_c$ (which is equal to $\omega(\sigma_c)\,d\sigma_c$), by the probability that all remaining (m-1) elements exceed $\sigma_c + d\sigma_c$ in strength (which is equal to $\left[1 - \Omega(\sigma_c)\right]^{m-1}$) and considering that failure can occur in any of the m bundles. This approach will be applied to glass reinforced plastic composites below.

Definition of Model Parameters

For the statistical model, the link dimension and the link strength distribution function are required. The former is defined by a shear lag type approximate analysis of the stress distribution in the vicinity of a broken end. The model is shown in Figure 2. Details of the analysis are presented in Appendix A. This yields the following result for the ineffective length, δ, normalized with respect to the fiber diameter:

$$\frac{\delta}{d_f} = \frac{1}{2}\left[\frac{\left(1 - v_f^{1/2}\right)}{v_f^{1/2}}\left(\frac{E_f}{G_b}\right)\right]^{1/2} \cosh^{-1}\left[\frac{1 + (1-\varphi)^2}{2(1-\varphi)}\right] \tag{8}$$

where

v_f = fiber volume fraction

E_f = fiber Young's modulus

G_b = binder shear modulus

φ = fraction of the undisturbed stress value below which fiber is considered to be ineffective.

Figure 3 shows the variation of fiber ineffective length with constituent moduli for various fiber concentrations. These ineffective lengths are relatively small; however, they are based upon an elastic analysis which

yields stresses as shown in Figure 4. It is clear that for many composites the matrix shear stresses will exceed the elastic limit of the material. The point at which the elastic limit is reached is indicated on each curve of Figure 4 for a matrix shear yield stress of one tenth the fiber strength. Since for high concentrations most of the curves are above the elastic limit, even for this comparatively high strength binder, further inelastic analysis is required. As a first approximation to the inelastic problem an approximate elastic-plastic analysis has been performed to assess the effect of inelasticity on ineffective length. This combination of linear elasticity to a given yield stress and then constant stress for all larger strains is a gross idealization of the binder stress strain curve, but it does enable an estimate of the nature of inelastic effects. The resulting effects are shown in Figure 5 where the elastic and elastic-plastic results for otherwise identical composites are compared, for a matrix yield stress of 5% of the fiber tensile strength. The increase in ineffective length is apparent and, as will be shown, detrimental.

With the ineffective length and, synonomously, the fiber link length defined, the statistical strength distribution of the links can be deduced from fiber test data. This process is detailed in Appendix B. The result is that if the fiber strength distribution, $g(\sigma)$, and the associated cumulative distribution function, $G(\sigma)$, are known for fibers of length, L, then the desired distribution function, $f(\sigma)$, for the links of length, δ, is given by:

$$f(\sigma) = \frac{g(\sigma)}{n}\left[1 - G(\sigma)\right]^{(1/n) - 1} \tag{9}$$

where $L = n\delta$

Thus, if for illustrative purposes, one treats fibers characterized by a Weibull (Ref. 7) distribution function:

$$g(\sigma) = L\alpha\beta\sigma^{\beta - 1} \exp\left(-L\alpha\sigma^{\beta}\right) \tag{10}$$

where α and β are the two parameters characterizing the distribution, it is found that:

$$f(\sigma) = \alpha \delta \beta \sigma^{\beta-1} \exp(-\alpha \delta \sigma^{\beta}) \tag{11}$$

Substitution of eqs. (8) and (11) into the results of the previous section defines the composite strength distribution function, $\lambda(\sigma_t)$. In particular the statistical mode, σ_t^*, is found by setting:

$$\frac{d\lambda}{d\sigma_t} = 0 \tag{12}$$

which yields:

$$\sigma_t^* = v_f (\alpha \delta \beta e)^{-1/\beta} \tag{13}$$

where α and β are the constants defining the link strength and are determined by experimental tests of fiber strength vs. length as described previously. δ is the ineffective length defined by a fiber shear stress analysis and e is the base of natural logarithms.

The results of the preceding sections are used in eq. (13) to compute composite strength. The predicted composite failure stress is plotted in Figure 6 for the range of ineffective lengths of one to one hundred fiber diameters. The range one to ten generally corresponds to the elastic predictions (see Figure 3) and the range ten to one hundred to the inelastic predictions. Also shown in Figure 6 are the effects of variations in fiber characteristics. Curves are presented to show the effect of an increase in the dispersion, as measured by a 10% change in β, and of a decrease in the reference strength as measured by a 10% change in $\alpha^{-1/\beta}$. The failure stresses shown neglect the effect of binder extensional stresses and hence a composite failure stress is obtained by multiplying the value for $v_f = 1.0$ (which is the stress based on fiber area alone) by the actual fiber volume fraction.

Implications of the Failure Model

One of the reasons for the existence of many tensile failure models is that, for gross behavior, there are many similarities in the predictions which are obtained from widely differing models. Consider first the influence of volume fraction upon strength. In eq. (13) the ineffective length is a function of fiber volume fraction, v_f. This function is given in eq. (8) which for defined constituents can be written as:

$$\frac{\delta}{d_f} = c_1 \left(\frac{1 - v_f^{1/2}}{v_f^{1/2}} \right)^{1/2} \tag{14}$$

and from eq. (13)

$$\sigma_t^* = \sigma_{ref} v_f \left(\frac{1 - v_f^{1/2}}{v_f^{1/2}} \right)^{-1/2\beta} \tag{15}$$

where σ_{ref} is a reference stress level which is a function of fiber and matrix properties.

This equation is plotted in Figure 7 (for $\beta = 7.7$, which is a typical value for commercial E-glass filaments) where it is compared with the rule of mixtures value, namely:

$$\sigma_t = \sigma_{ref} v_f \tag{16}$$

The tensile strength of the matrix has been neglected since it is usually of little importance in this sense except at low fiber volume fractions. The curve of eq. (15) does not go to unity at a fiber volume fraction of unity because the maximum packing density of fibers is a hexagonal array for uniform diameter fibers with $v_f = 0.904$. The proximity of the two curves indicates the hazard of inferring from agreement with experimental data that the analysis which generated one or the other curve is a correct model of the failure process.

The next problem is the question of selecting a reference fiber strength with which to make comparisons between composite performance

and expected composite performance. In treating fibers which are characterized statistically, the hazard of using a mean value should be quite apparent from the previous observations of the variation in fiber strength. Thus the strength value does not have a meaning unless there is a length value associated with it. Consider fibers characterized by eq. (10) and composed of n links of length δ, where $L = n\delta$, which links are characterized by:

$$f(\sigma) = \alpha \delta \beta \sigma^{\beta-1} \exp(-\alpha \delta \sigma^{\beta}) \tag{17}$$

The k^{th} moment of such a distribution function is defined by:

$$M_k = \int_0^{\infty} \sigma^k f(\sigma)\, d\sigma \tag{18}$$

The mean, $\bar{\sigma}$, and standard deviation, s, are defined in terms of this moment function as follows:

$$\bar{\sigma} = M_1 \tag{19}$$

$$s = \left[M_2 - M_1^2\right]^{1/2} \tag{20}$$

Substitution of (17) and (18) into (19) and (20) yields:

$$\bar{\sigma} = (\alpha \delta)^{-1/\beta} \Gamma(1 + 1/\beta) \tag{21}$$

$$s = (\alpha \delta)^{-1/\beta} \left[\Gamma(1 + 2/\beta) - \Gamma^2(1 + 1/\beta)\right] \tag{22}$$

Similarly, for fibers of length, L, eqs. (11), (18) and (19) yield the mean strength of such individual fibers, $\bar{\sigma}_L$, as:

$$\bar{\sigma}_L = (\alpha L)^{-1/\beta} \Gamma(1 + 1/\beta) \tag{23}$$

It is now possible to answer the question: what is the relationship between the composite strength (the statistical mode) and the mean strength of individual fibers of length, L? The answer is:

$$\frac{\sigma_t^*}{\bar{\sigma}_L} = \left(\frac{\delta}{L}\right)^{-1/\beta} \frac{(\beta \cdot e)^{-1/\beta}}{\Gamma(1 + 1/\beta)} \tag{24}$$

It is of interest to plot this strength ratio as a function of the fiber coefficient of variation which is obtained from eqs. (19) and (20) as:

$$\frac{s}{\bar{\sigma}} = \frac{\left[\Gamma(1 + 2/\beta) - \Gamma^2(1 + 1/\beta)\right]^{1/2}}{\Gamma(1 + 1/\beta)} \tag{25}$$

Note that for the Weibull distribution, this ratio is independent of fiber gage length. Simultaneous solution of eqs. (24) and (25) for selected values of L/δ is achieved by varying β. The results are plotted in Figure 8 where composite strength is plotted as a function of the fiber coefficient of variation, that is, the standard deviation divided by the mean value at that same length. Thus it is seen that in dealing with composites of length equal to one ineffective length, that is the basic bundle of fiber links of the model previously described, the mode of the bundle strength is slightly lower than the mean strength of individual fibers and departs from this value as the variation increases. The other curves show that as the length ratio increases, as is the case for reasonable specimens where the fiber length is large compared to the ineffective length, one would expect from this analysis that composite strength would be somewhat larger than the mean strength of fibers of the same length. And since these numbers are close to one, for coefficients of variation as large as 15%, it is easy to interpret the composite performance as having been equal to some fraction of the fiber performance. In general, the composite strength indicated here would not be achieved because the damage to the fibers during the fabrication process changes the population characterization. Curves of this type then have an important use in assessing how far the composite deviates from its potential strength value because of additional damage introduced after the time of the measurement of the

fiber strength. To emphasize the point, note that if one tests fibers of a given length and then tests a composite and compares the two strength values, these results indicate that, in general, the numbers are expected to be close together for fibers which do not have extreme variations. However, the fact that they are close together does not indicate that there is any understanding of the mode of failure. Thus, one may consider the experimental data to support the theory that failure is governed by the rule of mixtures or that failure is governed by this statistical fracture theory. Both yield similar results for this gross effect, yet the different models suggest different methods of increasing the composite strength. The importance of obtaining a correct model for the mechanics of fracture lies in the potential for achieving improved composites.

Experimental Program

The validity of the present model was investigated by a new experimental technique initially described in Ref. 4. This experimental program was directed toward making possible the observation of the failure mechanism during the actual loading process of the composite. The experimental model is shown in Figure 9 and consisted of a single layer of glass fibers imbedded in an epoxy matrix and loaded in tension parallel to the fibers. In the present extension of the study, fibers of a diameter which is large compared to commercial fibers were used. These were 3-1/2 mil E-glass fibers furnished through the courtesy of Narmco R&D. The fiber spacing was relatively close and the thickness of the specimen was only slightly larger than the diameter of the fiber. The overall specimen gage section dimensions were a 1/2" width, a 1" length and a thickness of about four thousandths of an inch. The fiber volume fraction was approximately 50%. The specimen was observed photoelastically during the test process in a fashion such that the unloaded specimen appears black. The major contributor to the photoelastic effect is the glass fibers and as they are loaded the fibers will brighten. Thus, when the fiber is at high load and appears bright a broken fiber will result in a zero stress region which is dark.

The fibers used in these specimens were tested individually at three different gage lengths and the results are plotted in Figure 10 in the form of average strength as a function of gage length. To indicate the effect of the matrix properties upon the composite, two test series were conducted utilizing epoxies which were very nearly identical except that one specimen had a flexibilizer added to it. This results in a decrease of the elastic modulus and an increase in the total strain to failure as shown in Figure 11. The test results are presented in Table 1. Typical photographic sequences of one specimen from each group are presented in Figures 12 and 13.

At less than 50% of the ultimate load, individual fiber fractures are observed. Since the fractured fiber in the vicinity of the fracture is unstressed the color returns to the original dark color. Thus, breaks appear as a short dark rectangular area with a thin white line across the center. The length of this dark area is the ineffective length of the fiber. As the load increases, the fibers fracture at random locations. Although there are stress concentrations in the vicinity of the breaks, the variation in fiber strength generally more than offsets the effect of such concentrations. Hence, the breaks occur randomly rather than cumulatively at the site of the initial break.

The effect of matrix properties on the character of the results is emphasized in Figure 14. Figure 14a is a reproduction of the picture at 99% of ultimate load of 3 1/2 mil E-glass fibers in an epoxy having a modulus of 0.48×10^6 psi. The fiber ineffective lengths are on the order of 10 diameters and distribution of fiber breaks is random. Figure 14b shows the similar specimen using a matrix material of modulus 0.28 million psi again taken at 99% of the maximum load. Here it is seen that (1) the ineffective lengths are substantially larger, being on the order of 30 diameters and (2) that the number of breaks are smaller and (3) the effect of stress concentrations is larger. Since the ineffective lengths are larger, it takes fewer of them to produce a weak cross section and hence failure of the composite. The role of the matrix in confining the detrimental effect of perturbations of the stress field which result from a fiber break are clearly evident. Thus, it is seen that although a ductile matrix is desirable from the point of view of alleviating

the stresses and preventing interface failure, and also for having a higher fracture toughness, a strong and stiff matrix would have a greater effect on confining the perturbations to the stress field thus producing a beneficial effect for the statistical failure model. Experiments using constituents which trade off these various factors are sorely lacking, and the proper evaluation of the relative merits of various failure models will require more experimental work. It is hoped that the experiments that have been described here can be extended to aid in this work.

Since the test data of Figure 10 yielded a straight line and since the Weibull distribution of eq. 10 would also produce such a straight line, as is apparent from eq. (23), the fiber test data can be used directly in the analytical model to predict composite strengths. This has been done and the results are presented in Figure 15 based on the fiber diameter of 3-1/2 mils for the experimental fibers used. The curve is linear on this logarithmic plot where the ineffective length ratios one to ten are appropriate to elastic matrix materials and the range 10 to 100 is the appropriate range for the inelastic results. The two test points previously described (average values from Table 1) are shown on this plot and it is seen that the two appear to have the trend of the analytical result but the strength levels are substantially below those shown. Several reasons exist for this; one important one being the fact that the fiber strength values of Figure 10 cannot be extrapolated to very short fibers since data (e. g. Ref. 8) show that the curve flattens out at very short lengths. Since the ineffective length, for a practical composite, is a very short fiber length, one must reconsider what amounts to an extrapolation of the straight line of Figure 10 down into the short fiber range. To do this consider some simple fiber populations; for example, the rectangular distribution shown in Figure 16a. Given this simple rectangular distribution function for the links in a fiber chain the cumulative distribution function is readily obtained as shown in Figure 16b. The chain representing a fiber containing n links would have a distribution function of the general shape shown in Figure 16c and its associated cumulative distribution function as shown in Figure 16d. However, it appears from data, for glass fibers for example, that the general characteristics of the distribution function indicates that the

bulk of the fibers fail within a finite band at high stress level and occasional fibers fail at small stress levels so that an idealized link distribution function would look more like that shown in Figure 17a. Here the bulk of the fibers are shown as in the preceeding simple rectangular distribution function with a small portion of the population isolated at a lower stress level. The effect on the cumulative distribution function for the fiber lengths is trivial. It departs from zero over the lower range as opposed to running along the axis to the stress σ_3 but the value p can be quite a small value. However, if one now looks at the effect of this small additional low stress group on the strength of a chain it is seen that there exists a distribution function which has two peaks, where the maximum value of the two peaks are as shown, and also the cumulative distribution function is rather drastically modified. The analysis defining these results is presented in Appendix B.

For p arbitrarily small there is some large n value which will sufficiently diminish the right hand peak of Figure 17C with respect to the left hand peak so that a long enough chain will soon have its strength dominated by the low stress level group of the population. Figure 18 shows the number of elements n required to make these two peaks equal to one another as a function of p, the fraction of the population in the low strength region. The number of elements required is a function of the ratio of the width of upper rectangular band, $\sigma_4 - \sigma_3$, to the width of the lower rectangular band, $\sigma_2 - \sigma_1$. Results are shown for three different values of this ratio. It can be seen that even for fractions of the population in the low strength region as low as 1% only several hundred elements are required before the lower peak equals the upper peak. The influence of the distribution of fibers between the two different regions is shown more clearly in Figure 19, in which the average fiber strength is plotted as a function of the fiber length where the distribution function for the individual elements is as shown in the lower left portion. Here the upper band is twice the width of the lower band and only 1% of the link elements are considered to be in the lower band. The result for the mean strength curve very closely simulates the experimentally observed bilinear distribution of strength versus length. It is considered significant that distributions of this form can reproduce the experimental

data. Evidently the prospects are encouraging for using such a distribution directly in the failure model that has previously been described.

The original example for the computation of composite strength was based on the use of a single straight line, such as the latter portion of this curve of Figure 19. It is clear that this can lead to an overestimate of the composite strength. Having demonstrated the ease with which the experimental fiber strength data can be simulated, it now remains to select an appropriate compound distribution function and use it in the previously derived statistical analysis. For example a Weibull distribution can be utilized in the following form:

$$f(\sigma) = p\alpha_1\delta\beta_1\sigma^{\beta_1 - 1} \exp(-\alpha_1\delta\sigma^{\beta_1}) + (1 - p)\alpha_2\delta\beta_2\sigma^{\beta_2 - 1}\exp(-\alpha_2\delta\sigma^{\beta_2}) \quad (26)$$

and the associated cumulative distribution function:

$$F(\sigma) = 1 - p \exp(-\alpha_1\delta\sigma^{\beta_1}) - (1 - p)\exp(-\alpha_2\delta\sigma^{\beta_2}) \quad (27)$$

It is seen that for p equals either zero or one, the result reduces to a simple Weibull distribution and for any p value this compound distribution can be used in the preceding equations in exactly the same fashion as the simple one was with only the sacrifice of algebraic simplicity.

Conclusions Regarding Tensile Failure

The tensile model indicates that randomly distributed fiber fractures occur well below the ultimate composite strength. The statistical strength characterization of the fibers determines the frequency of these fiber breaks. The strength of the composite is determined by this and by the efficiency with which the matrix limits the effect of the perturbation of the local stress field produced by a fiber break. The need for statistical characterization of fibers and for consideration of matrix deformations is strongly indicated. A new

experimental technique for the evaluation of the tensile failure process has been presented and the results support the analytical model.

The analysis does not include all possible detrimental effects and hence it is perhaps best to view the results as indications of the potential for advanced structural composites. These potentials are the major conclusions of the present study. Simply stated, the conclusion is that high strength fibers used in an appropriate matrix can yield composites having tensile strengths usually attained only in very short lengths of very small diameter filaments.

COMPRESSIVE STRENGTH

The problem considered is the compressive strength of a fibrous composite formed by the set of parallel fibers imbedded in an otherwise homogeneous matrix. The composite is considered to be subjected to compressive load parallel to the fiber direction. It has been suggested by Dow (Ref. 9) that the mode of failure for such a composite is the small wavelength buckling of the fibers in a fashion analogous to the buckling of a column on an elastic foundation. One of the motivations for such a composite failure model is indicated in Figure 20. Photoelastic stress patterns are shown for three individual glass fibers imbedded in an epoxy matrix which has been cured at a temperature of about 250°F. As is well known, the shrinkage of the epoxy from its cure temperature down to room temperature results in the frequently observed elastic instability of the glass fiber. E-glass fibers of five, three and one half, and one half mil diameter in three separate blocks of epoxy are shown. It is clear from the repeated stress pattern that a buckling failure has occurred. All three blocks consist of the same epoxy subjected to the same cure conditions. The only apparent difference between specimens is the difference in amplitude and wavelength of buckling. The shrinkage of the epoxy resin provides a convenient means for applying a compressive strain to this glass fiber and observing the resultant instability. The analytical model of a column on an elastic foundation indicates that the buckling wavelength of a circular column would be directly proportional to the fiber diameter (see Ref. 10). The three fibers shown here are all in identical epoxy matrices and hence the foundation modulus, although unknown, can be considered to be the same in all cases. Thus, it would be expected that the buckling wavelength would be linearly dependent upon the fiber diameter. Figure 21 shows the measured experimental results. Here the buckle wavelength is plotted against the fiber diameter on logarithmic paper so that a linear relationship between the two appears as a 45° line on this graph. The three test points shown in Figure 20 are plotted along with a best fit 45° line. The agreement between this analytical curve and the test data indicates at least qualitatively that there is some justification for considering the elastic instability mode as the failure mode for the glass fibers.

The problem of quantitatively evaluating this instability failure for multiple fibers imbedded in the homogeneous matrix is not as straightforward. The analytical model considered in the present analysis is shown in Figure 22. A series of parallel fibers are treated as a two dimensional problem, so that the model consists of plates of thickness h separated by a matrix of dimension 2c. Each fiber is subjected to a compressive load, P, the fiber length is given by the dimension, L. Now, two possibilities are considered for the failure mode here. First, the fibers may buckle in opposite directions in adjacent fibers as shown on the left portion of Figure 22 and the so-called extension mode occurs. This mode receives its name from the fact that the major deformation of the matrix material is an extension in the direction perpendicular to the fibers. The model considers that the fibers are stiff relative to the matrix and that shear deformations in the fiber can be neglected relative to those in the matrix. The second possibility is shown on the right portion of the figure where adjacent fibers buckle in the same wavelength and in phase with one another, so that the deformation of the matrix material between adjacent fibers is primarily a shear deformation. Hence, the shear mode label for this potential mode. The energy method for evaluation of the buckling stress for these modes has been utilized, where the procedure is to consider the composite stressed to the buckling load and then to compare the strain energy in this compressed but straight deformation pattern to a deformation pattern following an assumed buckling shape under the same load. Thus, a change in the strain energy of the composite consisting of the strain energy change in the fiber, ΔV_f, and the strain energy change in the binder, ΔV_b, can be compared to the change in the potential energy associated with the shortening of the distance between the applied loads at the end of the fibers, ΔT. The condition for instability is given by equating the strain energy change to the work done by the external loads during buckling. Details of the analysis are presented in Appendix C.

The results for the compressive strength, σ_c, for the extension mode is given by:

$$\sigma_c = 2v_f \left[\frac{v_f E_b E_f}{3(1 - v_f)}\right]^{1/2} \tag{28}$$

The result for the shear mode is given by:

$$\sigma_c = \frac{G_b}{1 - v_f} \tag{29}$$

These results are plotted in Figure 23 for E-glass fibers imbedded in an epoxy matrix. The compressive strength of the composite is plotted as a function of the fiber volume fraction, v_f. The two curves represent the two failure modes considered. It is seen that for the low fiber volume fractions the extension mode is the lower stress, while for high volume fractions of fibers the shear mode predominates. The compressive strength of reasonable glass reinforced plastic containing fiber volume fractions on the order of 0.6 to 0.7 is seen to be on the order of 450 to 600 ksi. Values of this magnitude do not appear to have been measured for any realistic specimens. However, the achievement of a strength of half a million psi in a composite of this type would require an average shortening of greater than 5%. For the epoxy materials used, such a shortening would result in a decrease in the effective shear stiffness of the binder material because the proportional limit of the matrix would be exceeded. It does appear necessary to modify the analysis to consider inelastic deformation of the matrix material. A first simple approximation to this has been provided by replacing the binder modulus in the formulas previously shown by a modulus which varies linearly for the epoxy from its elastic value at 1% strain to a zero value at 5% strain. The result of this assumption is the curve labeled inelastic in Figure 23. Here it is seen that for very high fiber volume fractions the strength is bounded and, although higher than any results obtained to date, they are not unreasonably high. The results of this study are presented in a somewhat different form in Figure 24 where the average compressive strain at failure is plotted as a function of the fiber volume fraction for composites having two different ratios of fiber Young's modulus to binder shear modulus. Curves for the two failure modes, that is extension and shear, are presented. The strength of the composite is obtained simply from these curves by multiplying the shortening by the product of fiber volume fraction and fiber Young's modulus. These curves again indicate that the shear instability mode is predominant over the

major range of interest for these ratios of fiber to binder moduli. Also indicated is the fact that a substantial difference in the result is achieved for a change in the ratio of fiber to binder moduli. Thus, the factor of 2 utilized in the example here results in almost a factor of 2 on the results for the shear mode. Thus, changes in the effective value of the shear stiffness of the binder when stressed beyond the elastic limit of the material can have a substantial effect on the predicted value of the composite.

The results presented so far are based on strain energy computations which have involved some assumptions regarding the displacements, and hence, it is no longer valid to treat the stress obtained as an upper bound of the buckling stress. In order to investigate the nature of the approximation made in the strain energy a more precise model must be considered. This is done by treating the boundary value problem defined by considering an elastic domain subjected to sinusoidal normal displacements on the boundary. The strain energy in the binder material is evaluated by considering this strip as a two-dimensional elastic domain. The equilibrium equation expressed in terms of displacements can be used to obtain a solution to this problem by following an approach used by Timoshenko (Ref. 10) for the related traction boundary value problem. That is the displacements μ_x and μ_y can be assumed to be arbitrary functions of y multiplied by trigonometic functions of the longitudinal direction x. Substitution of these displacements into the equilibrium equations can be shown to yield an ordinary differential equation for the function of y. The constants in this solution are evaluated by considering the boundary conditions on the displacements. From this the strain energy can be found and this strain energy can be used in the expression shown previously to obtain a true bound on the compressive critical buckling stress. This can be done under the assumption that the fiber is sufficiently rigid so that shear deformations of the fiber can be neglected. It is also possible to relax even this constraint and consider two adjacent elastic domains; one representing the binder and one representing the fiber and to have boundary conditions in the form of continuity of displacements and normal tractions across the surface rather than in the form of prescribed sinusoidal deformations. This approach requires further study.

Another assessment of the results of the present analysis with experiment can be obtained by utilizing existing results (Reference 11) for hollow glass fiber composites. These results are shown in Figure 25. Here a set of short compression columns fabricated from hollow glass fibers imbedded in an epoxy matrix and tested in compression are plotted in the form of the ratio of the strength to density ratio for a hollow glass fiber composite normalized with respect to a composite containing solid E-glass fibers with the same binder volume fraction. Each experimental point here is for a composite containing a 30% binder on a volume basis and each point represents the average of at least 5 tests of nominally identical specimens. The fiber radius ratio, that is the ratio of the inner to the outer radii of the hollow glass fibers, is the independent variable. The analysis indicates that the stress to density curve would increase monotonically with the fiber radius ratio over the range of $\alpha < 0.9$. It is seen that the experimental data appear to have the analytical result as an upper bound.

Conclusions Regarding Compressive Strengths

It appears that the compressive strength of a fibrous composite loaded in a direction parallel to the fibers is governed by an instability mode analogous to the buckling of a column on an elastic foundation. An analysis to assess the quantitiative effect of the influence of constituent properties upon this buckling stress has been presented.

The compression model indicates that the matrix shear stiffness is the material property which has the most significant effect on composite compressive strength. The choice of the failure mode is supported qualitatively by experimental results for the compressive strength of hollow glass fiber composites.

It appears that the use of matrix materials having shear moduli which are moderate rather than small with respect to the fiber Young's modulus can yield composites, of high modulus fibers, which have extremely high compressive strength. Of course the binder must have these values at the high strains associated with the very high composite compressive strengths.

REFERENCES

1. Machlin, E. S., "Status Report on Non-Metallic Fibrous Reinforced Metal Composites" Status Report, Contract NOw 61-0209-c, Sept. 1961.

2. Jech, R. W., McDanels, D. L. and Weeton, J. W., "Fiber Reinforced Metallic Composites," Proceedings of the 6th Sagamore Ordnance Materials Research Conference, August 1959.

3. Parratt, N. J., "Defects in Glass Fibers and Their Effect on the Strength of Plastic Mouldings," Rubber and Plastics Age, March 1960.

4. Rosen, B. W.: "Tensile Failure of Fibrous Composites," AIAA Journal (scheduled for publication in Nov./Dec. 1964).

5. Gücer, D. E. and Gurland, J. "Comparison of the Statistics of Two Fracture Modes," Journal of the Mechanics and Physics of Solids pp. 365-373, 1962.

6. Daniels, H. E., "The Statistical Theory of the Strength of Bundles of Threads," Proceedings of the Royal Society, p. 405, 1945.

7. Weibull, W., "A Statistical Distribution Function of Wide Applicability," Journal of Appl. Mech., Sept. 1951.

8. Metcalfe, A. G.; and Schmitz, G. K.: "Effect of Length on the Strength of Glass Fibers," ASTM 1964 preprint No. 87, June, 1964.

9. Dow, N. F. and Gruntfest, I. J.: "Determination of Most Needed Potentially Possible Improvements in Materials for Ballistic and Space Vehicles," GE TIS 60SD389, June, 1960.

10. Timoshenko, S.: "Theory of Elastic Stability," Section 21, McGraw-Hill, New York, 1936.

11. Rosen, B. W.; and Ketler, A. E. Jr.: "Hollow Glass Fiber Reinforced Plastics," GE-TIS R63SD41, May, 1963.

12. Sadowsky, M. A., "Transfer of Force by High-Strength Flakes in a Composite Material," Watervliet Aresonal, TR WVT-RR-6105-R, June, 1961.

13. Dow, N. F., "Study of Stresses Near a Discontinuity in a Filament-Reinforced Composite Metal," Space Mechanics Memo #102, GE Space Sciences Laboratory, January 1961.

APPENDIX A

EFFECTIVE FIBER LENGTH

The definition of ineffective length, δ, involves the determination of the shear stress distribution along the fiber-matrix interface. An analysis of this problem has been presented for idealized fiber shapes without the effect of surrounding fibers (ref. 12). An approximate solution similar to that of ref. 13 is presented herein. The model used is shown in fig. 2 and consists of a fiber surrounded by a matrix which in turn is imbedded within a composite material. The latter has the average or effective properties of the composite under consideration. This configuration is subject to axial stress and a shear lag type analysis is utilized to estimate the stresses.

Load is applied parallel to the fiber direction. The fiber is assumed to carry only extension and the matrix to transmit only shear stresses. No stress is transmitted axially from the fiber end to the average material. Shear stresses in the average material are considered to decay in a negligible distance from the inclusion interface.

For equilibrium of a fiber element in the axial direction:

$$\tau + \frac{r_f}{2} \frac{d\sigma_f}{dz} = 0 \tag{A-1}$$

where

τ = shear stress in matrix material

σ_f = axial stress in fiber

For equilibrium of the composite in the axial direction:

$$\left(\frac{r_f}{r_a}\right)^2 \sigma_f + \left(\frac{r_a^2 - r_b^2}{r_a^2}\right)\sigma_a = \bar{\sigma} \tag{A-2}$$

where

σ_a = axial stress in average material

$\overline{\sigma}$ = applied axial stress

The displacements in the fiber, u_f, and in the average material, u_a, define the binder shear strain, δ, as follows:

$$u_a - u_f = (r_b - r_f)\,\gamma \tag{A-3}$$

Differentiating eq. (A-3) twice and using the stress-strain relations yields:

$$\frac{1}{E_a}\frac{d\sigma_a}{dz} - \frac{1}{E_f}\frac{d\sigma_f}{dz} = \frac{r_b - r_f}{G_b}\frac{d^2\tau}{dz^2} \tag{A-4}$$

where

E_a = effective Young's modulus of the composite

E_f = Young's modulus of the fiber

G_b = shear modulus of the binder

Differentiating eq. (A-2) and substituting the result and eq. (A-1) into eq. (A-4) yields:

$$\frac{d^2\tau}{dz^2} - \eta^2\tau = 0 \tag{A-5}$$

where

$$\eta^2 = \frac{2G_b}{E_f (r_b - r_f)(r_f)}\left[1 + \frac{E_f}{E_a}\left(\frac{r_f^2}{r_a^2 - r_b^2}\right)\right]$$

The solution to eq. (A-5) is of the form

$$\tau = A \sinh \eta z + B \cosh \eta z$$

The boundary conditions are:

$$\tau\,(o) = 0$$

$$\sigma_f(\ell) = 0$$

$$\therefore\ B = 0$$

$$A = \frac{G_b\,\bar{\sigma}\,r_a^{\,2}}{\eta E_a\,(r_b - r_f)\,(r_a^{\,2} - r_b^{\,2})\,\cosh\,\eta\,\ell}$$

and

$$\tau = \frac{G_b\,\bar{\sigma}\,r_a^{\,2}\,\sinh\,\eta\,z}{\eta\,E_a\,(r_b - r_f)\,(r_a^{\,2} - r_b^{\,2})\,\cosh\,\eta\,\ell} \qquad \text{(A-6)}$$

From eqs. (A-11) and (A-16):

$$\sigma_f = -\frac{\bar{\sigma}\,r_a^{\,2}\,E_f}{\left[E_a\,(r_a^{\,2} - r_b^{\,2}) + E_f\,r_f^{\,2}\right]}\left(\frac{\cosh\,\eta\,z}{\cosh\,\eta\,\ell} - 1\right) \qquad \text{(A-7)}$$

Consider $r_a >> r_b$

$$\therefore\ \eta^2 \approx \frac{2G_b}{r_f E_f\,(r_b - r_f)} \qquad \text{(A-8)}$$

and from eq. (A-18):

$$\sigma_f = -\frac{\bar{\sigma}\,E_f}{E_a}\left[\frac{\cosh\,\eta\,z}{\cosh\,\eta\,\ell} - 1\right] \qquad \text{(A-9)}$$

The maximum axial stress is

$$\sigma_f\,(o)\Big|_{\ell\,\to\,\infty} = \frac{\bar{\sigma}\,E_f}{E_a} \qquad \text{(A-10)}$$

Using the results of this elastic analysis, the stress ratio, φ, is evaluated from the ratio of the stress at a distance δ from the end of a given fiber to the stress at the midpoint of a very long fiber. The stress at a point at distance δ from a fiber end is:

$$\sigma_f (\ell - \delta) = - \frac{\bar{\sigma} E_f}{E_a} \left[\frac{\cosh \eta(\ell - \delta)}{\cosh \eta \ell} - 1 \right] \qquad \text{(A-11)}$$

The fiber efficiency, φ, at this point is therefore defined by:

$$\varphi = \frac{\sigma_{z1} (\ell - \delta)}{\sigma_{z1} (o) \Big|_{\ell \to \infty}} = 1 - \cosh \eta \delta + \tanh \eta \ell \sinh \eta \delta \qquad \text{(A-12)}$$

for large ℓ:

$$\tanh \eta \ell = 1$$

$$\therefore \varphi = 1 - \cosh \eta \delta + (\cosh^2 \eta \delta - 1)^{1/2} \qquad \text{(A-13)}$$

From which

$$\cosh \eta \delta = \frac{1 + (1 - \varphi)^2}{2 (1 - \varphi)} \qquad \text{(A-14)}$$

and

$$\frac{\delta}{d_f} = \frac{1}{2} \left[(v_f^{-1/2} - 1) \frac{E_f}{G_b} \right]^{1/2} \cosh^{-1} \left[\frac{1 + (1 - \varphi)^2}{2 (1 - \varphi)} \right] \qquad \text{(A-15)}$$

For the purposes of this analysis a value of $\varphi = 0.9$ is considered, and δ is evaluated for this stress ratio value Thus, effective length is that portion of the fiber in which the average axial stress is greater than 90% of the stress which would exist for infinite fibers. Fig. 3 shows the variation of ineffective length with constituent moduli for various fiber concentrations.

APPENDIX B

STATISTICAL MODELS FOR FIBER STRENGTH

A fiber is considered to consist of a chain of links. Any consistent combination of link length and link strength distribution which combine to reproduce the fiber strength data are acceptable. With link length defined as in Appendix A, the statistical distribution of link strength is obtained from experimental fiber strength distributions. Consider links characterized by the distribution function $f(\sigma)$ and the associated cumulative distribution $F(\sigma)$ where:

$$F(\sigma) = \int_0^{\sigma} f(\sigma)\, d\sigma \tag{B-1}$$

For n such links forming a chain which fails when the weakest link fails the distribution function $g(\sigma)$ for the chain is defined by:

$$g(\sigma) = nf(\sigma)\left[1 - F(\sigma)\right]^{n-1} \tag{B-2}$$

From this, the cumulative distribution function, $G(\sigma)$ for the fibers is obtained:

$$G(\sigma) = \int_0^{\sigma} g(\sigma)\, d\sigma \tag{B-3}$$

$$\therefore G(\sigma) = 1 - \left[1 - F(\sigma)\right]^{n} \tag{B-4}$$

The solution of the inverse problem is desired. That is, given the fiber data, $g(\sigma)$ and $G(\sigma)$, define the link data for a link length, δ. From eq. (B-4):

$$F(\sigma) = 1 - \left[1 - G(\sigma)\right]^{1/n} \tag{B-5}$$

and thus from (B-1) and (B-5):

$$f(\sigma) = \frac{g(\sigma)}{n}\left[1 - G(\sigma)\right]^{(1/n) - 1} \tag{B-6}$$

As an example, consider fibers characterized by a strength distribution of the Weibull (ref. 7) type:

$$g(\sigma) = L \alpha \beta \sigma^{\beta - 1} \exp(-L \alpha \sigma^{\beta}) \qquad \text{(B-7)}$$

This form has been shown to characterize the experimental length L, to strength, σ, relationship of fibers. Using equation (B-7) in (B-3) and (B-6) yields:

$$f(\sigma) = \alpha \delta \beta \sigma^{\beta - 1} \exp(-\alpha \delta \sigma^{\beta}) \qquad \text{(B-8)}$$

where:

$$L = n\delta$$

The constants α and β can be evaluated by using experimental strength-length data. To do this, consider the mean fiber strength, $\overline{\sigma}_f$ for a given length which, is defined by:

$$\overline{\sigma}_f = \int_0^{\infty} \sigma g(\sigma) \, d\sigma \qquad \text{(B-9)}$$

Substituting eq. (B-7) into (B-9) and integrating yields:

$$\overline{\sigma}_f = (L\alpha)^{-1/\beta} \Gamma\left(1 + \frac{1}{\beta}\right) \qquad \text{(B-10)}$$

A logarithmic plot of the available data for $\overline{\sigma}_f$ as a function of L will define the constants. Such a plot is presented in fig. 10. The linearity of the data support the choice of the distribution function given by eq. (B-7).

The constant β is an inverse measure of the dispersion of material strength. Values of β between two and four correspond to brittle ceramics, while a value of twenty is appropriate for a ductile metal (ref. 5). The constant α, as seen from eq. (20), defines a characteristic stress level, $\alpha^{-1/\beta}$.

Most experimental data for glass fibers (e.g. ref. 8) indicate that a plot of the type shown in fig. 10 should be bi-linear with the smaller slope in the very short gage-length region. The following work is the analysis of a simple model designed to illustrate a possible cause for this bi-linear behavior. The model is presented to indicate how the behavior of such fibers in a composite can be treated by the method of ref. 4.

Consider a rectangular distribution as shown in fig. 16a. For this:

$$\begin{aligned} f(\sigma) &= \frac{1}{b-a} && a \le \sigma \le b \\ f(\sigma) &= 0 && \begin{cases} \sigma < a \\ \sigma > b \end{cases} \end{aligned} \qquad \text{(B-11)}$$

From (B-1) and (B-11):

$$\begin{aligned} F(\sigma) &= \frac{\sigma - a}{b-a} && a \le \sigma \le b \\ F(\sigma) &= 0 && \sigma < a \\ F(\sigma) &= 1 && \sigma > b \end{aligned} \qquad \text{(B-12)}$$

Substituting (B-11) and (B-12) into eq. (B-2) yields:

$$g(\sigma) = 0 \qquad \begin{cases} \sigma < a \\ \sigma > b \end{cases}$$

$$g(\sigma) = \frac{n}{b-a}\left(\frac{b-\sigma}{b-a}\right)^{n-1} \qquad a \le \sigma \le b \qquad \text{(B-13)}$$

The mode of $g(\sigma) = \sigma^* = a$

Next consider the double rectangular distribution shown in fig. 17a. Here:

$$
\left.
\begin{array}{lll}
f(\sigma) = 0 & & \sigma < \sigma_1 \\
f(\sigma) = \dfrac{p}{\sigma_2 - \sigma_1} & & \sigma_1 \le \sigma \le \sigma_2 \\
f(\sigma) = 0 & & \sigma_2 < \sigma < \sigma_3 \\
f(\sigma) = \dfrac{1 - p}{\sigma_4 - \sigma_3} & & \sigma_3 \le \sigma \le \sigma_4 \\
f(\sigma) = 0 & & \sigma > \sigma_4
\end{array}
\right\} \qquad \text{(B-14)}
$$

Substituting eqs. (B-14) into eq. (B-1) yields:

$$
\left.
\begin{array}{lll}
F(\sigma) = 0 & & \sigma < \sigma_1 \\
F(\sigma) = p\left(\dfrac{\sigma - \sigma_1}{\sigma_2 - \sigma_1}\right) & & \sigma_1 \le \sigma \le \sigma_2 \\
F(\sigma) = p & & \sigma_2 < \sigma < \sigma_3 \\
F(\sigma) = p + (1 - p)\left(\dfrac{\sigma - \sigma_3}{\sigma_4 - \sigma_3}\right) & & \sigma_3 \le \sigma \le \sigma_4 \\
F(\sigma) = 1 & & \sigma > \sigma_4
\end{array}
\right\} \qquad \text{(B-15)}
$$

For the chain, substitution of eqs. (B-14) and (B-15) into eq. (B-2) yields:

$$
\left.
\begin{aligned}
g(\sigma) &= 0 && \sigma < \sigma_1 \\
g(\sigma) &= \frac{np}{\sigma_2 - \sigma_1}\left[1 - p\left(\frac{\sigma - \sigma_1}{\sigma_2 - \sigma_1}\right)\right]^{n-1} && \sigma_1 \le \sigma \le \sigma_2 \\
g(\sigma) &= 0 && \sigma_2 < \sigma < \sigma_3 \\
g(\sigma) &= \frac{n(1-p)}{\sigma_4 - \sigma_3}\left[(1-p) - (1-p)\left(\frac{\sigma - \sigma_3}{\sigma_4 - \sigma_3}\right)\right]^{n-1} && \sigma_3 \le \sigma \le \sigma_4 \\
g(\sigma) &= 0 && \sigma > \sigma_4
\end{aligned}
\right\} \quad \text{(B-16)}
$$

This yields the distribution function shown in Figure 17c. The values of the two peaks are:

$$g(\sigma_1) = \frac{np}{\sigma_2 - \sigma_1} \quad \text{(B-17)}$$

$$g(\sigma_3) = \frac{n(1-p)^n}{\sigma_4 - \sigma_3} \quad \text{(B-18)}$$

It is seen that the mode changes from σ_3 to σ_1 at some value of n. The value at which they are equal is plotted in fig. 18 and is obtained by setting:

$$g(\sigma_1) = g(\sigma_3) \quad \text{(B-19)}$$

From eqs. (B-7) to (B-9):

$$n = \frac{\log\left[p\left(\frac{\sigma_4 - \sigma_3}{\sigma_2 - \sigma_1}\right)\right]}{\log(1-p)} \quad \text{(B-20)}$$

The average strength for a given length fiber composed of n links taken from the population characterized by eqs. (B-4) is found as follows:

$$\bar{\sigma} = \int_0^\infty \sigma\, g(\sigma)\, d\sigma \quad \text{(B-21)}$$

$$\therefore \quad \bar{\sigma} = \int_{\sigma_1}^{\sigma_2} \frac{n\sigma p}{\sigma_2 - \sigma_1}\left[1 - p\left(\frac{\sigma - \sigma_1}{\sigma_2 - \sigma_1}\right)\right]^{n-1} d\sigma + \tag{B-22}$$

$$\int_{\sigma_3}^{\sigma_4} \frac{n\sigma (1 - p)^n}{\sigma_4 - \sigma_3} \left(\frac{\sigma_4 - \sigma}{\sigma_4 - \sigma_3}\right)^{n-1} d\sigma$$

which yields

$$\bar{\sigma} = \left[\sigma_1 - \sigma_2 (1 - p)^n\right] + \frac{\sigma_2 - \sigma_1}{p (n + 1)} \left[1 - (1 - p)^{n+1}\right] + \tag{B-23}$$

$$(1 - p)^n \sigma_3 + \frac{\sigma_4 - \sigma_3}{n + 1} (1 - p)^n$$

Eq. (B-23) is plotted in fig. 19 for selected values of p and σ_2. It is seen that the bi-linear distribution is very well simulated.

APPENDIX C

COMPRESSIVE STRENGTH OF FIBROUS COMPOSITES

The compressive strength of a fibrous composite is evaluated by treating the elastic stability of a two-dimensional array of layers of fiber and matrix material. The fibers are considered to be relatively stiff as compared to the binder and hence shear deformations of the fiber are neglected. Instability will be evaluated by utilizing the energy method. The change in strain energy for the fiber, ΔV_f, and the binder, ΔV_b, as the composite changes from a compressed but unbuckled configuration to the buckled state will be equated to the work, ΔT, done by the fiber loads. Thus,

$$\Delta V_f + \Delta V_b = \Delta T \tag{C-1}$$

For the two dimensional case the load per running inch on each fiber can be expressed as the product of fiber stress, σ_f, and fiber thickness, h:

$$P = \sigma_f h \tag{C-2}$$

The procedure then is to assume various buckle patterns and find the lowest buckling load. If all terms in the strain energy are appropriately considered each of these buckling stresses will provide an upper bound; and the lowest of these values may be taken as a buckling load. The cases to be considered herein are the two cases shown in Figure 22 where the buckling pattern in all fibers is of the same wavelength with adjacent fibers either in or out of phase with one another. The mixture of the two can be expected to have a buckling stress larger than the smaller load for the two individual modes. Each fiber will be assumed to buckle into the sinusoidal pattern expressed by the following series in v, the displacement in the y direction:

$$v = \sum_n a_n \sin \frac{n\pi x}{L} \tag{C-3}$$

For the extension mode, the tranverse strain is assumed to be independent of the y direction so that:

$$\epsilon_y = \frac{v}{c} \tag{C-4}$$

and

$$\sigma_y = E_b \frac{v}{c} \tag{C-5}$$

The changes in strain energy associated with the axial and shear stresses are considered negligible with respect to those due to the transverse stresses. Thus

$$\Delta V_b = \frac{1}{2} \int_v \sigma_y \epsilon_y \, dv \tag{C-6}$$

Substituting eqs. (C-3) to (C-5) into (C-6) yields:

$$\Delta V_b = \frac{E_b L}{2c} \sum_n a_n^2 \tag{C-7}$$

From ref. 10 (in the present nomenclature)

$$\Delta V_f = \frac{\pi^4 E_f h^3}{f8\ L^3} \sum_n n^4 a_n^2 \tag{C-8}$$

and

$$\Delta T = \frac{P\pi^2}{4L} \sum_n n^2 a_n^2 \tag{C-9}$$

Substituting eqs. (C-7) to (C-9) into (C-1):

$$P = \frac{\pi^2 E_f h^3}{12 L^2} \frac{\sum_n n^4 a_n^2 + \frac{24 L^4 E_b}{\pi^4 ch^3 E_f} \sum_n a_n^2}{\sum_n n^2 a_n^2} \tag{C-10}$$

Expression (C-10) is a minimum for one value of n, say m, hence

$$\sigma_{f_{cr}} = \frac{\pi^2 E_f h^2}{12 L^2} \left[m^2 + \frac{24 L^4 E_b}{\pi^4 ch^3 E_f} \left(\frac{1}{m^2} \right) \right] \tag{C-11}$$

Since m is large it may be treated as a continuous variable and eq. (C-11) can be minimized by setting

$$\frac{\partial \sigma_{f_{cr}}}{\partial m^2} = 0 \tag{C-12}$$

This yields

$$\sigma_{f_{cr}} = 2 \left[\frac{v_f E_b E_f}{3 (1 - v_f)} \right]^{1/2} \tag{C-13}$$

where

$$v_f = \frac{h}{h + 2c} \tag{C-14}$$

and for the composite stress, σ_c,

$$\sigma_c = v_f \sigma_{f_{cr}}$$

$$\therefore \sigma_c = 2 v_f \left[\frac{v_f E_b E_f}{3 (1 - v_f)} \right]^{1/2} \tag{C-15}$$

The critical strain, ϵ_{cr}, can be evaluated from eq. (C-13). Thus,

$$\epsilon_{cr} = 2 \left[\frac{v_f}{3 (1 - v_f)} \right]^{1/2} \left(\frac{E_b}{E_f} \right)^{1/2} \tag{C-16}$$

The shear instability mode is evaluated in a similar fashion. Here the displacements of all fibers are assumed to be of the same amplitude and in phase with one another. The shear strains are assumed to be a function of only the longitudinal coordinate, In the binder:

$$\gamma_{xy} = \frac{\partial u_y}{\partial x} + \frac{\partial u_x}{dy} \tag{C-17}$$

Since the transverse displacement is independent of the transverse coordinate, y:

$$\left.\frac{\partial u_y}{\partial x}\right|_b = \left.\frac{du_y}{dx}\right|_f \tag{C-18}$$

Since the shear strain is independent of y:

$$\frac{du_x}{dy} = \frac{1}{2c}\left[u_x(c) - u_x(-c)\right] \tag{C-19}$$

Since the fiber shear deformation is negligible:

$$u_x(c) = \frac{h}{2}\left.\frac{du_y}{dx}\right|_f \tag{C-20}$$

Substituting (C-19) into (C-18):

$$\frac{du_x}{dy} = \frac{h}{2c}\left.\frac{du_y}{dx}\right|_f \tag{C-21}$$

Substituting (C-21) and (C-18) into (C-17):

$$\gamma_{xy} = \left(1 + \frac{h}{2c}\right)\left.\frac{du_y}{dx}\right|_f \tag{C-22}$$

and

$$\tau_{xy} = G_b \gamma_{xy} \tag{C-23}$$

The changes in strain energy associated with the extensional stresses are considered negligible for this case. Thus:

$$\Delta V_b = \frac{1}{2} \int_v \tau_{xy} \gamma_{xy} \, dV \tag{C-24}$$

Substituting eqs. (C-3), (C-22) and (C-23) into (C-24) yields:

$$\Delta V_b = G_b c \left(1 + \frac{h}{2c}\right)^2 \left(\frac{\pi^2}{2L}\right) \sum_n a_n^2 n^2 \tag{C-25}$$

Using eq. (C-25) in place of eq. (C-7) in eq. (C-1) and proceeding as for the extension mode,

$$\sigma_{f_{cr}} = \frac{G_b}{v_f (1 - v_f)} + \frac{\pi^2 E_f}{12} \left(\frac{mh}{L}\right)^2 \tag{C-26}$$

Since L/m is the buckle wavelength, the second term in eq. (C-26) is small for wavelengths large compared with the fiber diameter, and the buckling stress is given approximately by:

$$\sigma_{f_{cr}} = \frac{G_b}{v_f (1 - v_f)} \tag{C-27}$$

and

$$\sigma_c = \frac{G_b}{1 - v_f} \tag{C-28}$$

$$\epsilon_{cr} = \frac{1}{v_f (1 - v_f)} \left(\frac{G_b}{E_f}\right) \tag{C-29}$$

The lower of the values given by eqs. (C-15) and (C-28) is the best estimate for the compressive strength.

Table 1
Thin Fibrous Composite Tensile Tests

Specimen Number	Maximum Number of Breaks	Maximum Load	Number of Fibers	Fiber Area (in^2)	Maximum Fiber Stress (ksi)
B1	37	210	125	1.272×10^{-3}	165.1
B2	31	222	130	1.323	167.8
B3	34	221	130	1.323	167.0
B4	13	207	131	1.333	155.3
B5	24(36)*	197	129	1.313	150.0
				Average stress	161.0
				Standard deviation	7.1
C1	21	195	125	1.272×10^{-3}	153.3
C2	28	181	124	1.262	143.4
C3	19(37)*	184	126	1.283	143.4
C4	33	196	126	1.283	152.8
C5	--	200			
C6	22	206	128	1.303	158.1
C7	20	203	122	1.242	163.4
				Average stress	152.4
				Standard deviation	7.1

* Number in parentheses observed after maximum load.

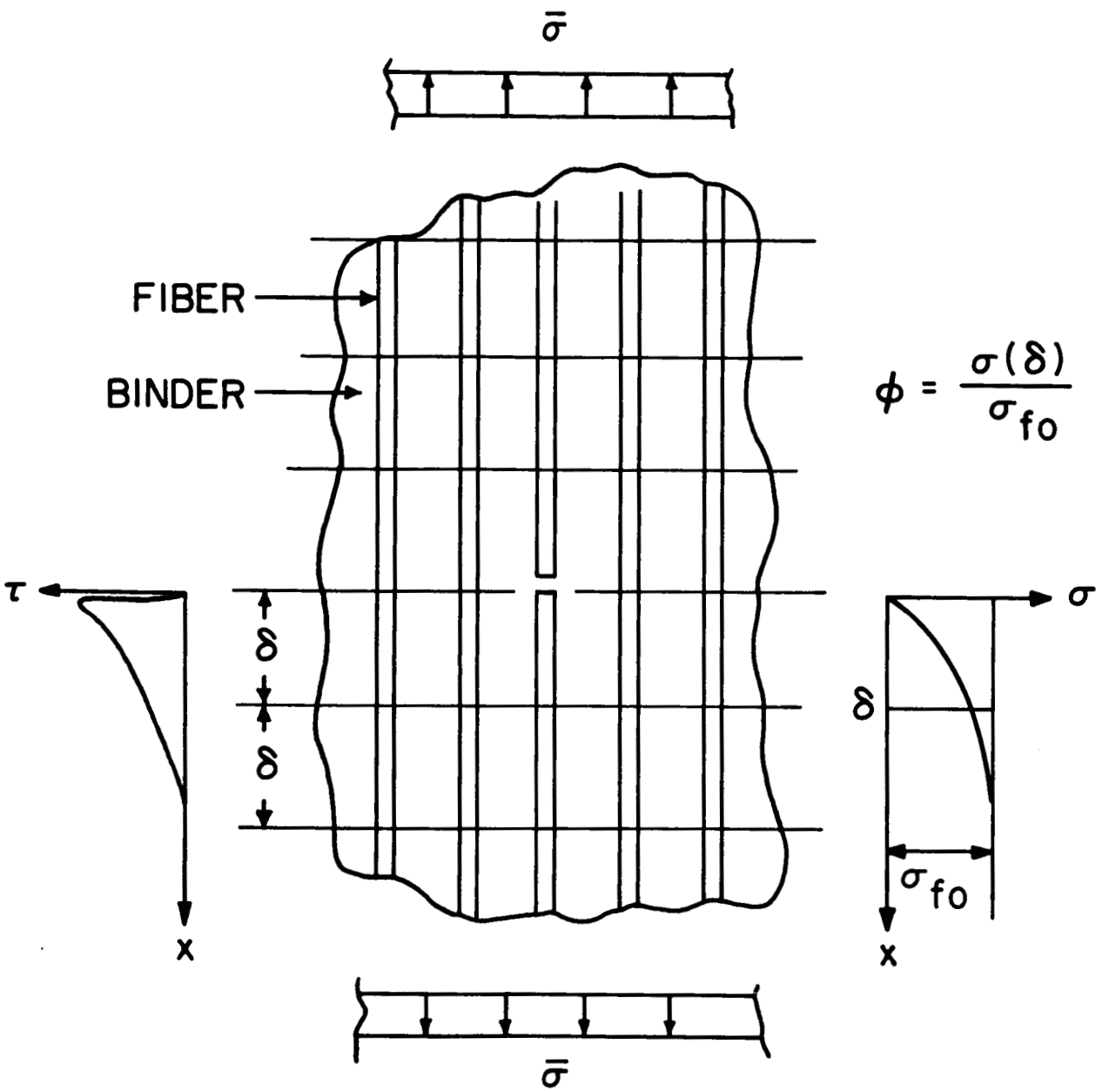

Figure 1. Fiber Reinforced Composite - Tensile Failure Model.

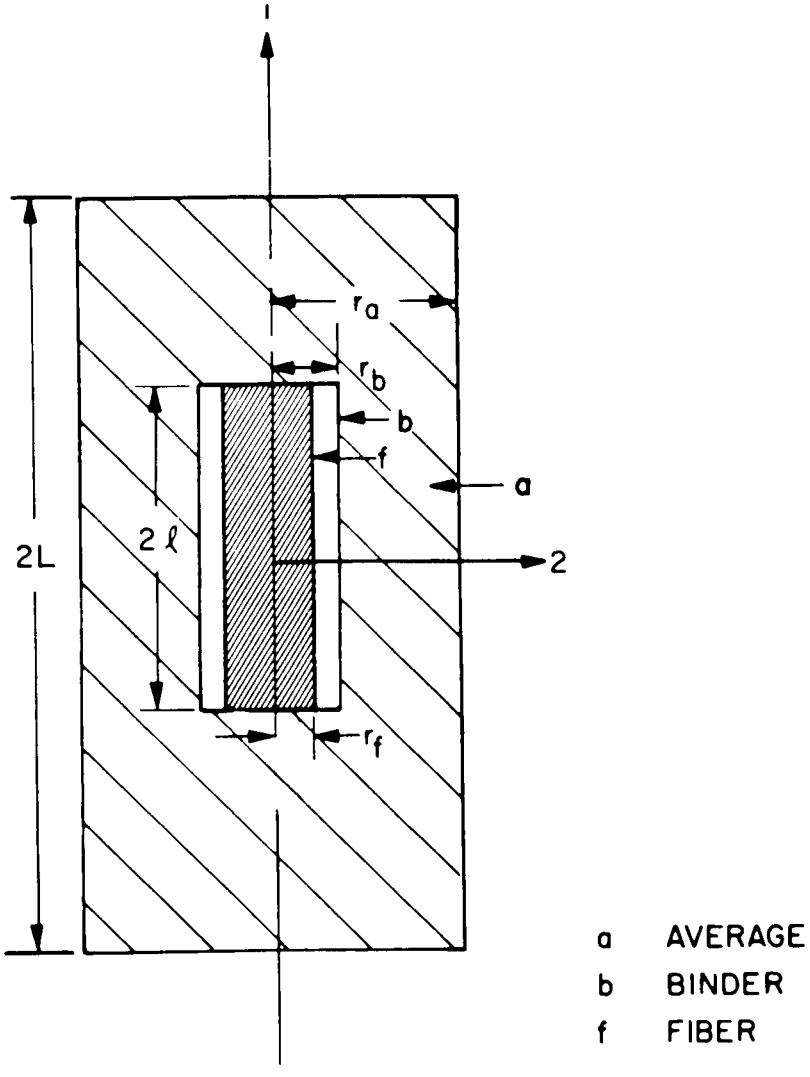

Figure 2. Model for Evaluation of Stresses at Fiber Ends

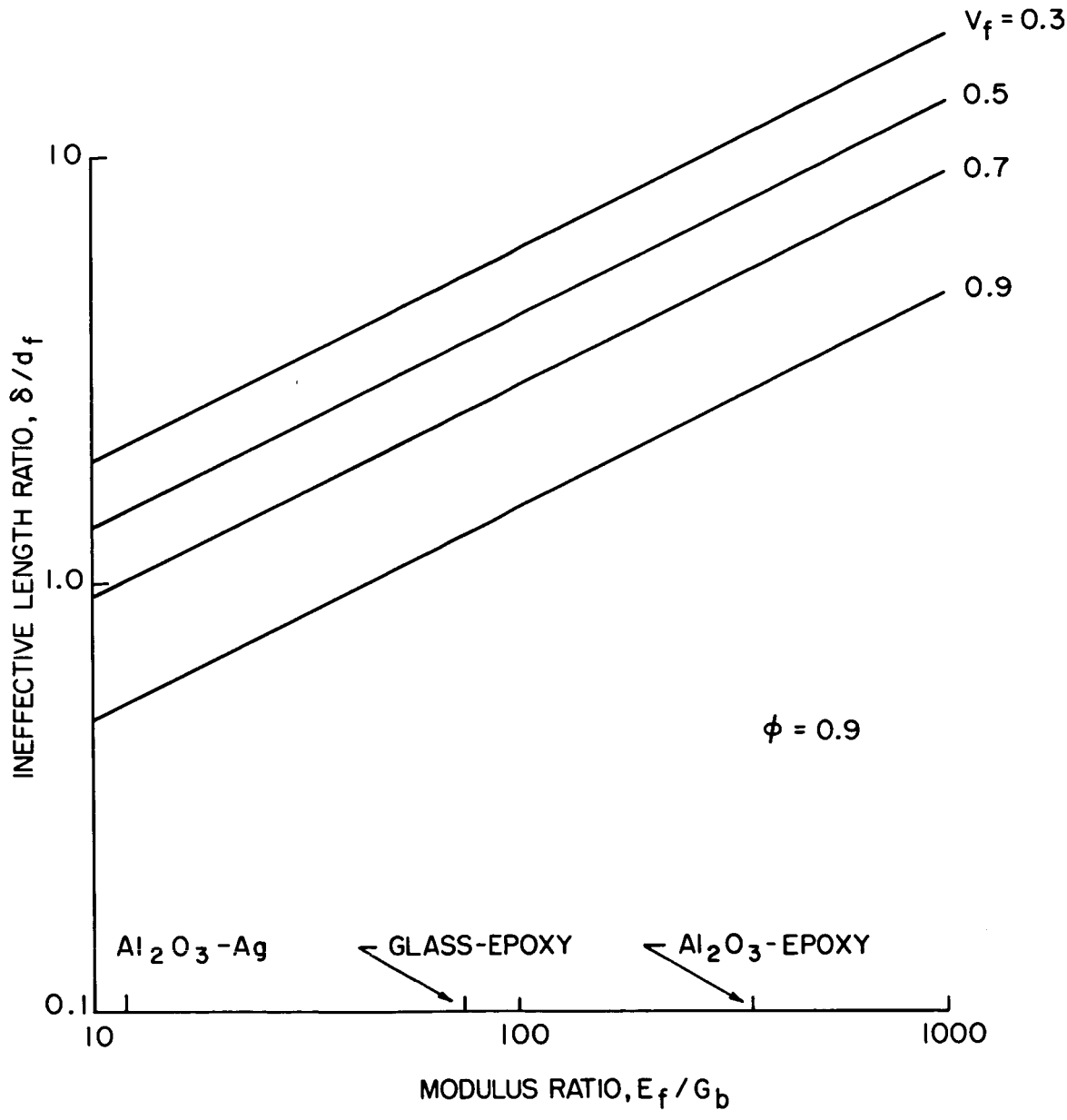

Figure 3. Ineffective Length of Fibers in Composites.

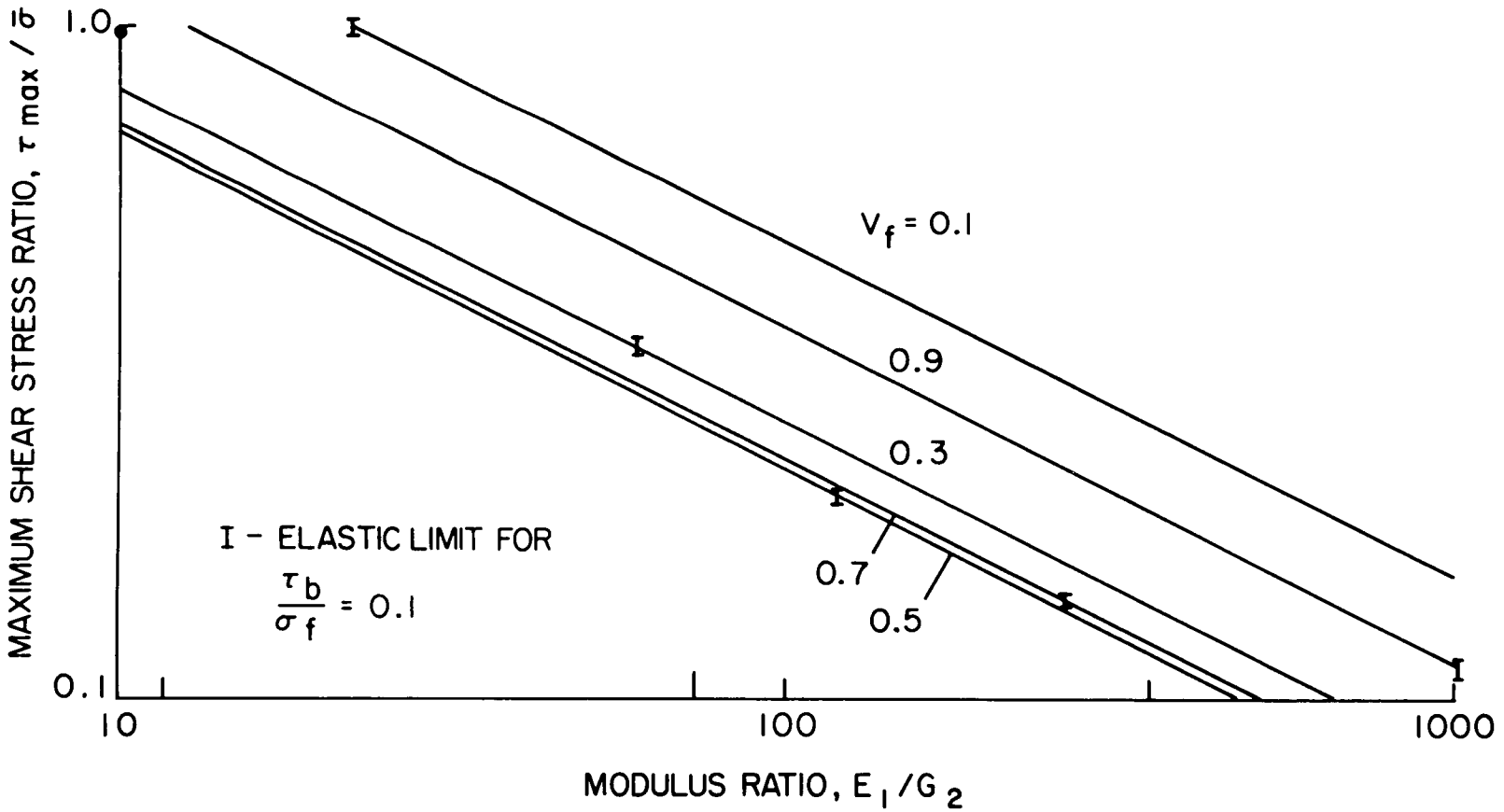

Figure 4. Maximum Fiber-Matrix Interface Shear Stress

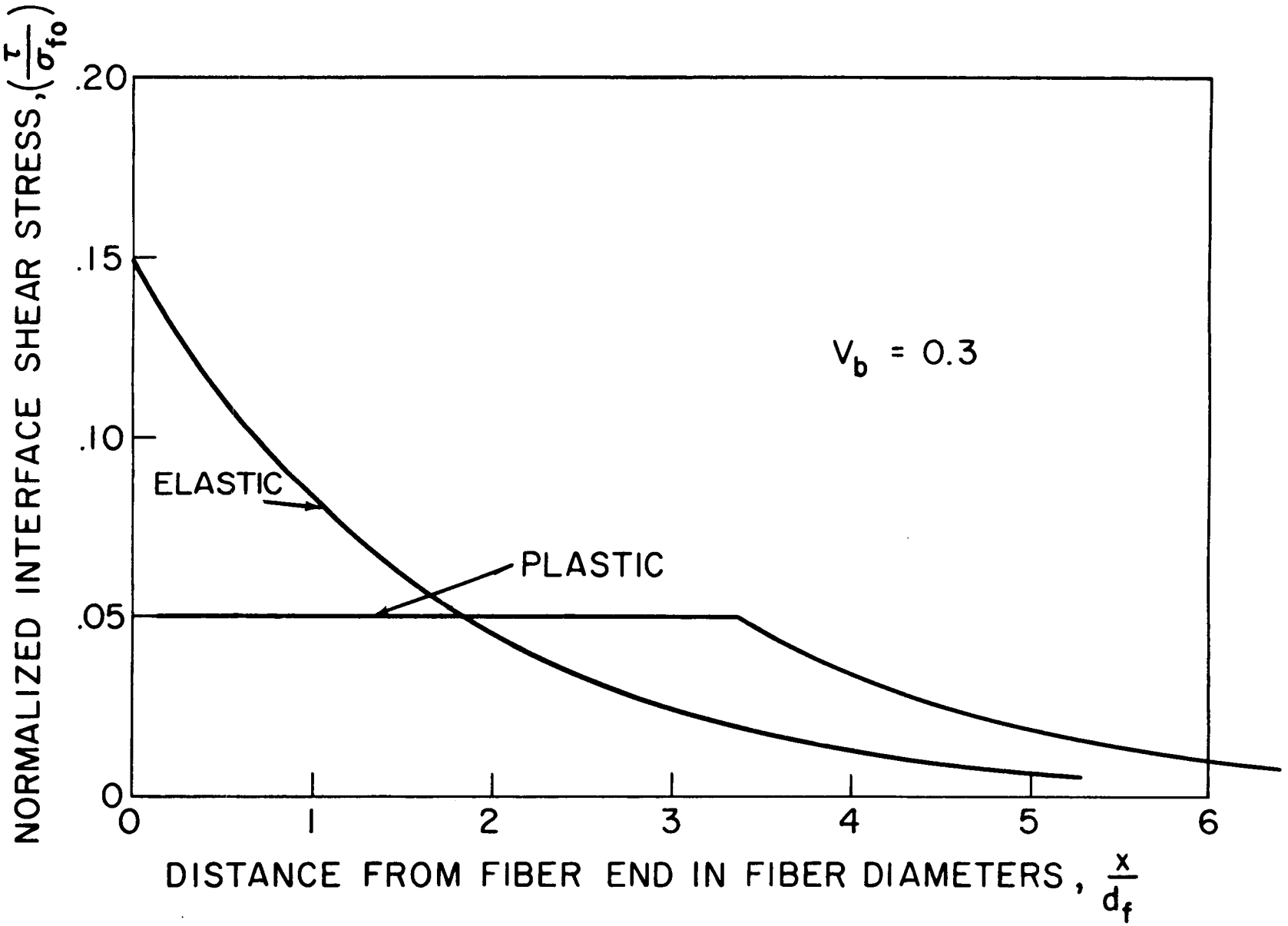

Figure 5. Variation of Interface Shear Stress and Fiber Extensional Stress for Glass Fibers in a Matrix having an Elastic-Plastic Stress-Strain Curve

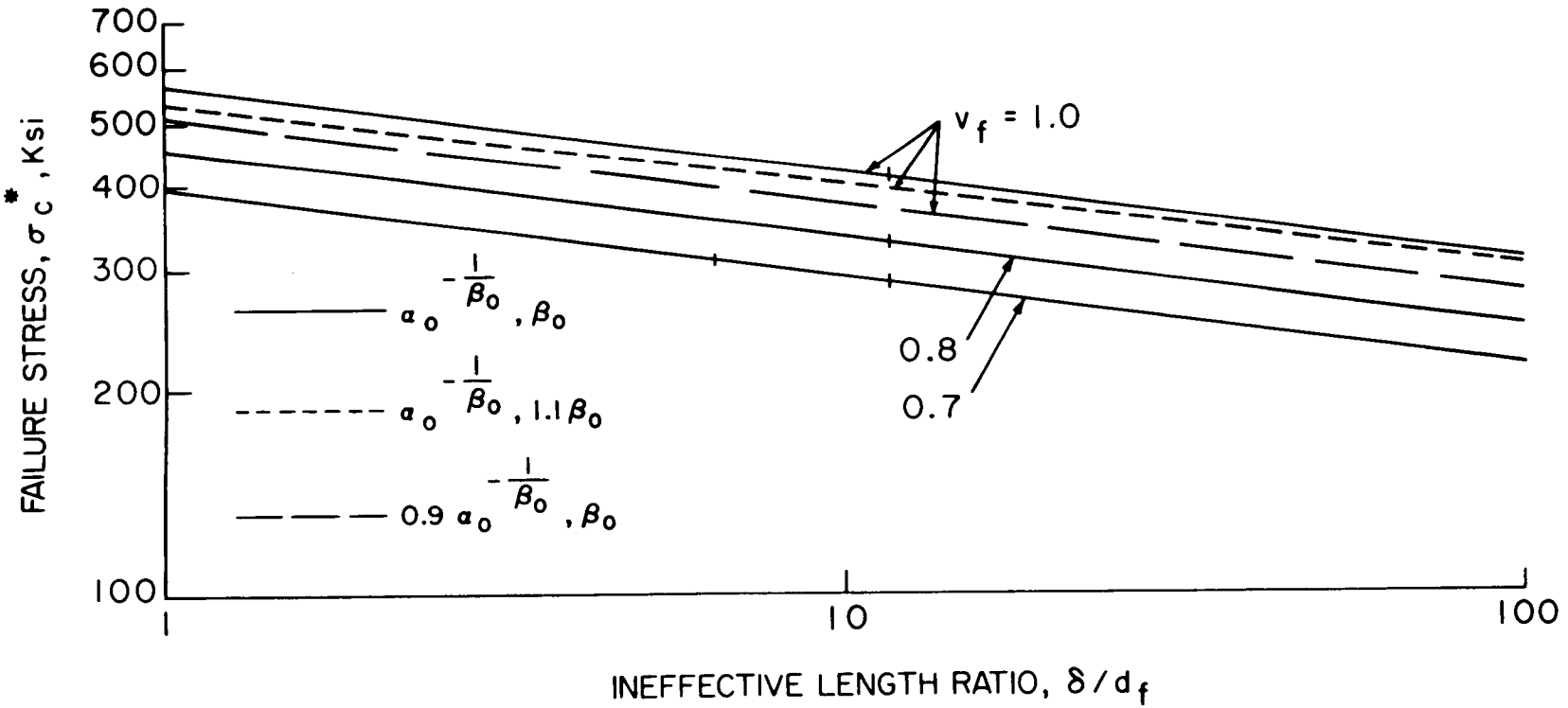

Figure 6. Statistical Mode of Glass Fiber-Plastic Composite Failure Stress

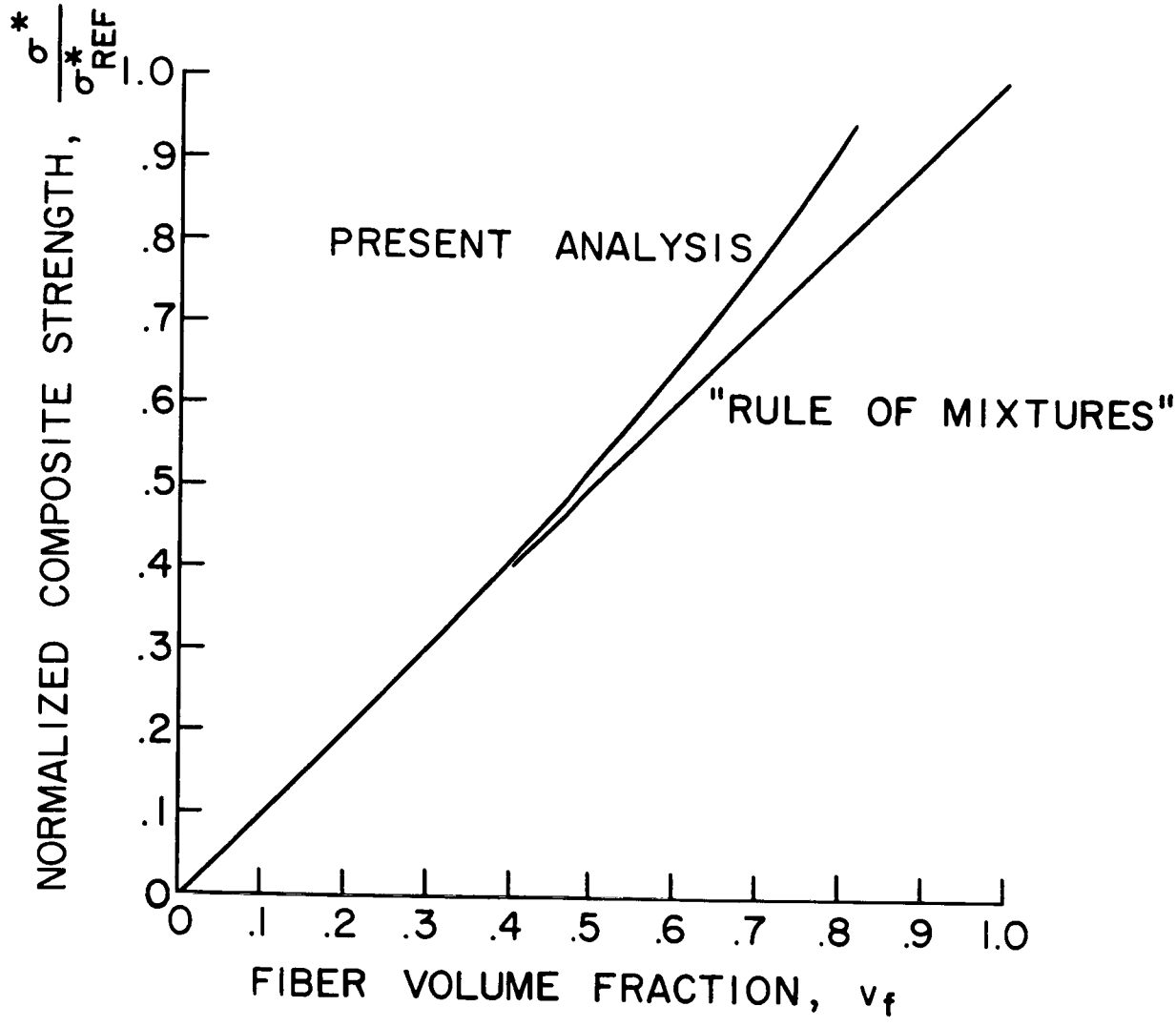

Figure 7. Variation of Composite Tensile Strength with Fiber Volume Fraction for Statistical Failure Model and for "Rule of Mixtures Model.

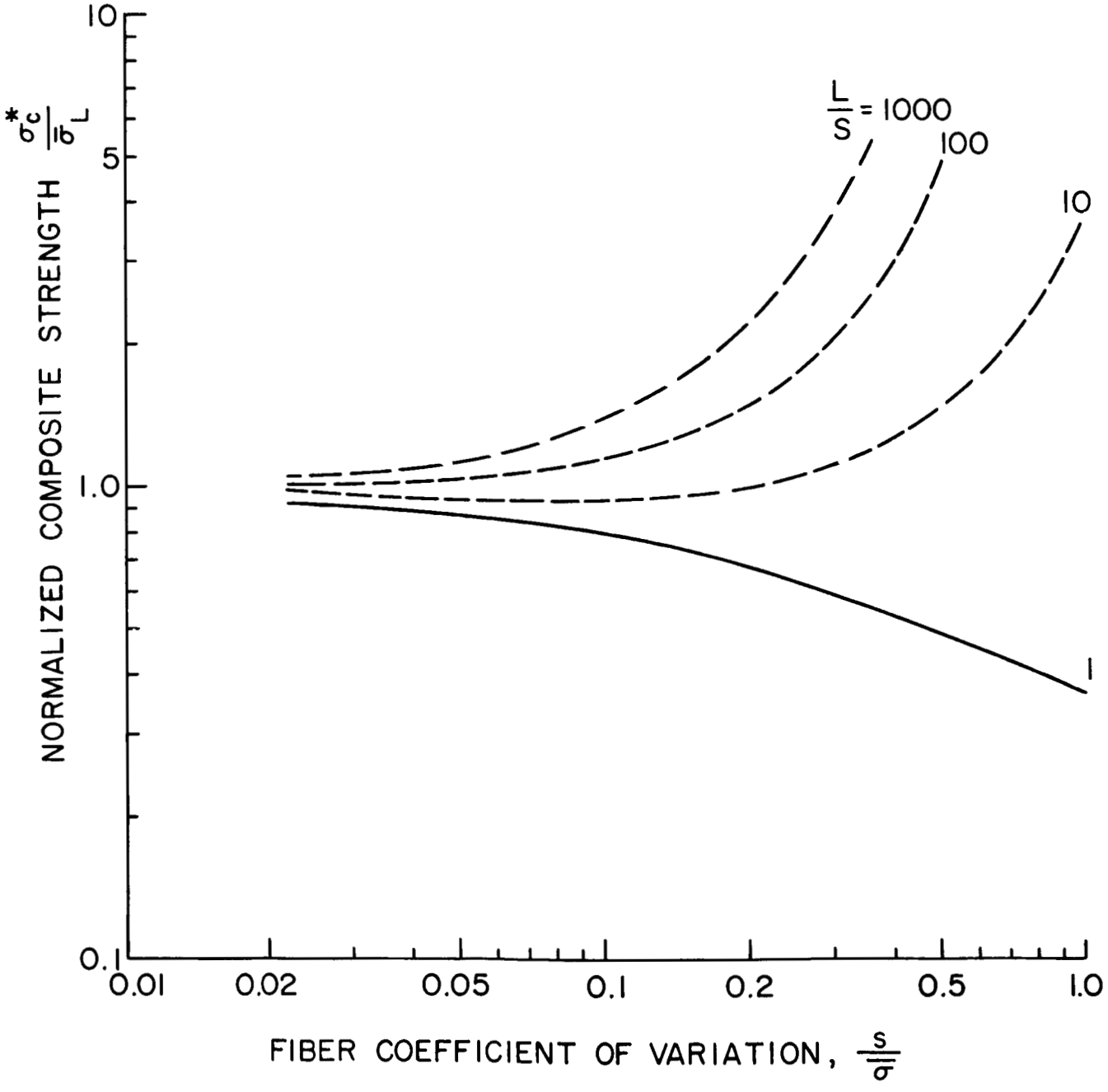

Figure 8. Effect of Fiber Coefficient of Variation and Reference Fiber Length (the statistical mode) to Mean Fiber Strength.

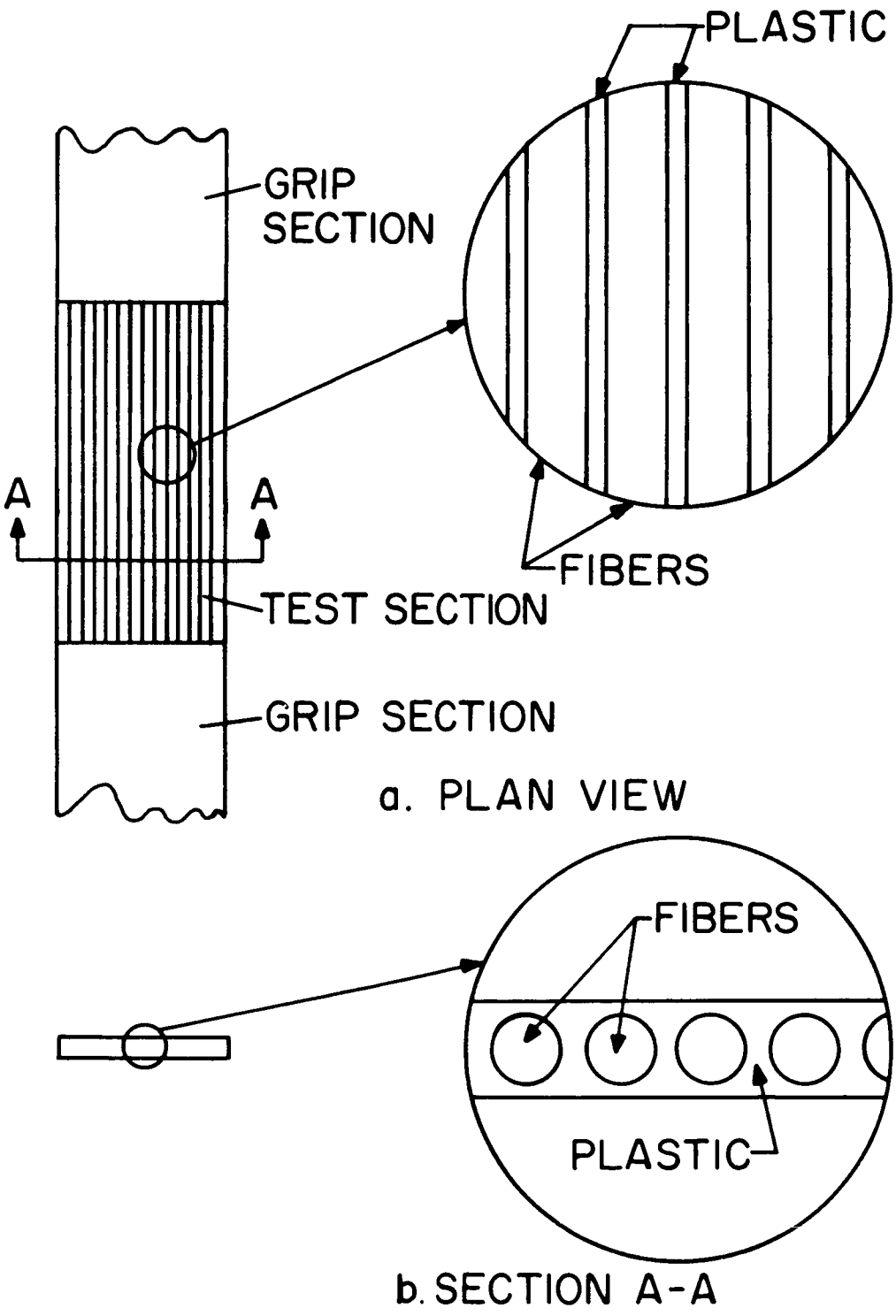

Figure 9. Experimental Tensile Failure Specimen.

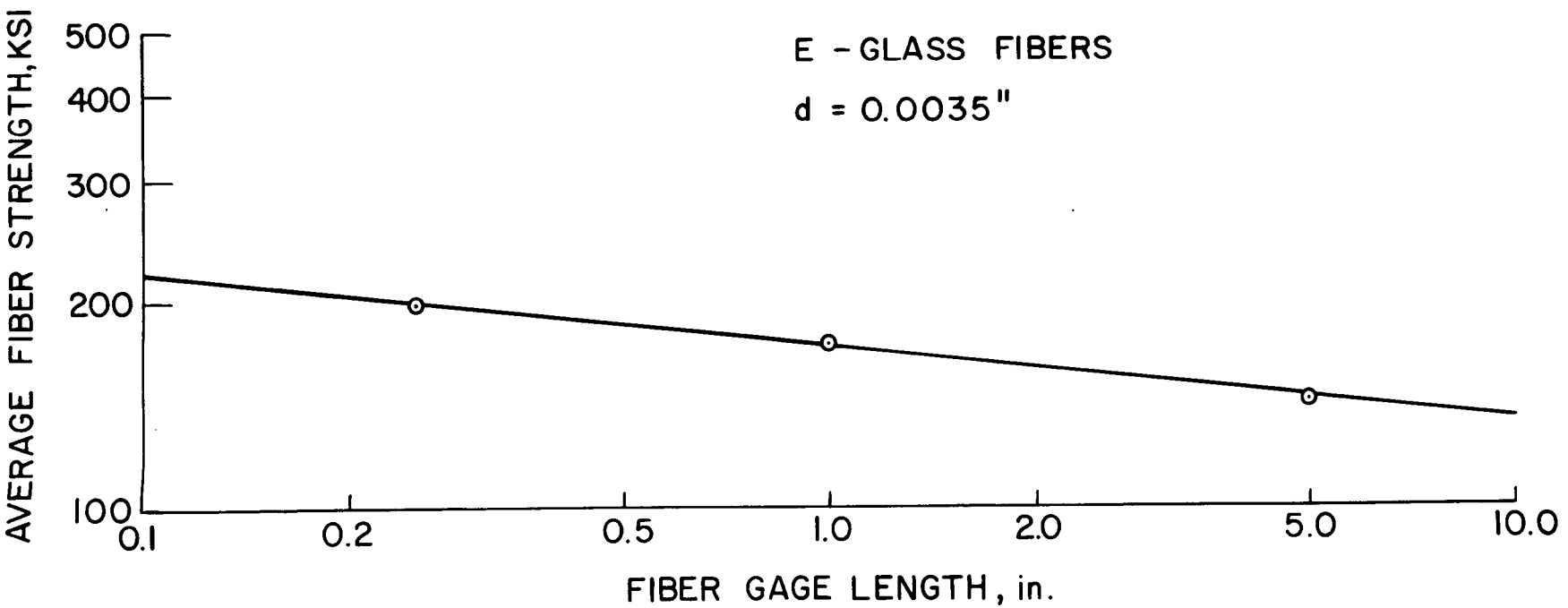

Figure 10. Effect of Length on Mean Fiber Strength.

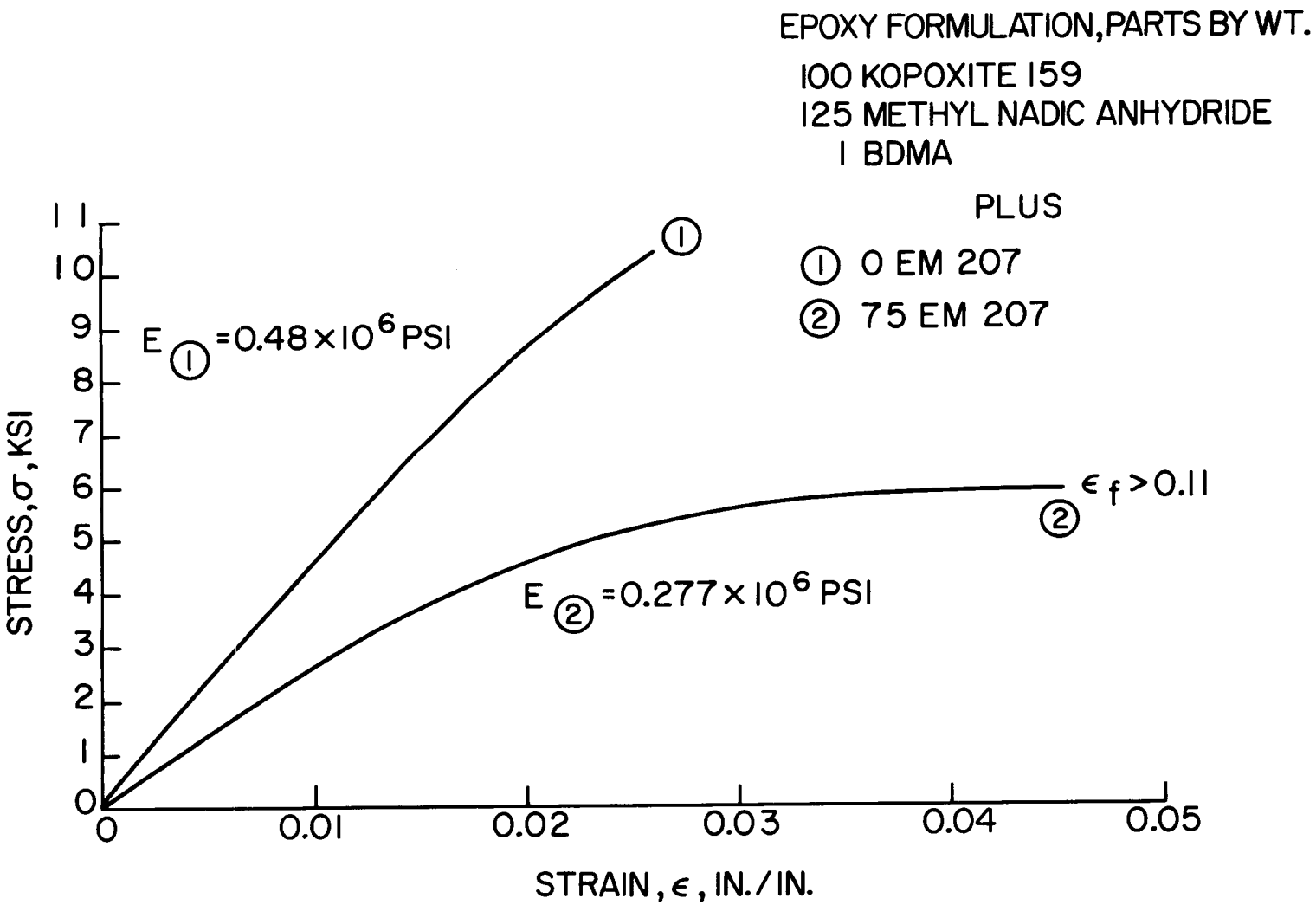

Figure 11. Experimental Stress-Strain Curves for Two Epoxy Materials.

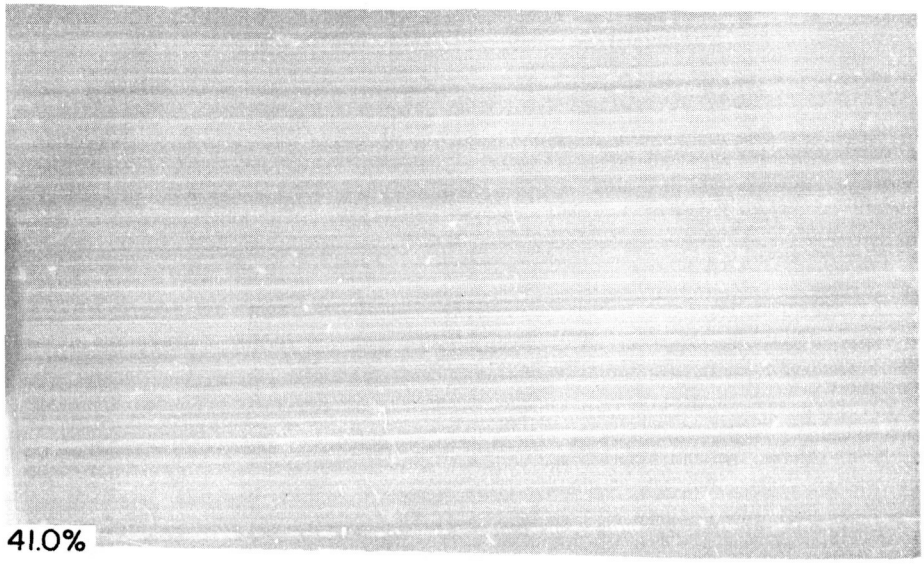

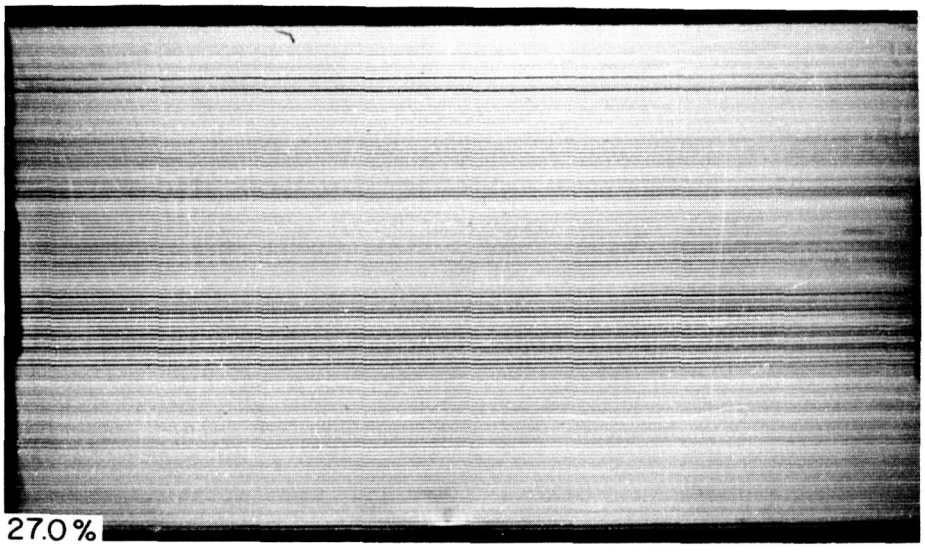

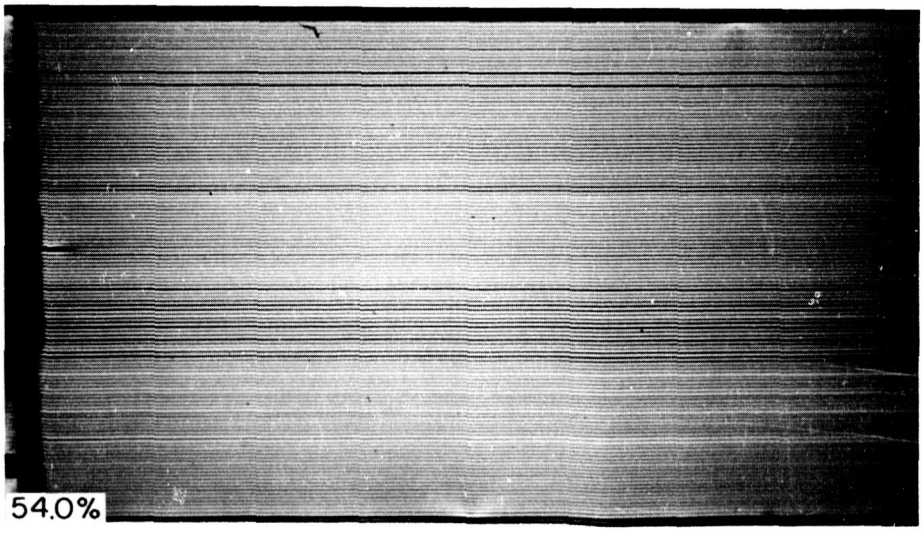

Figure 12. Failure Sequence of Specimen Having E_b = 0.48

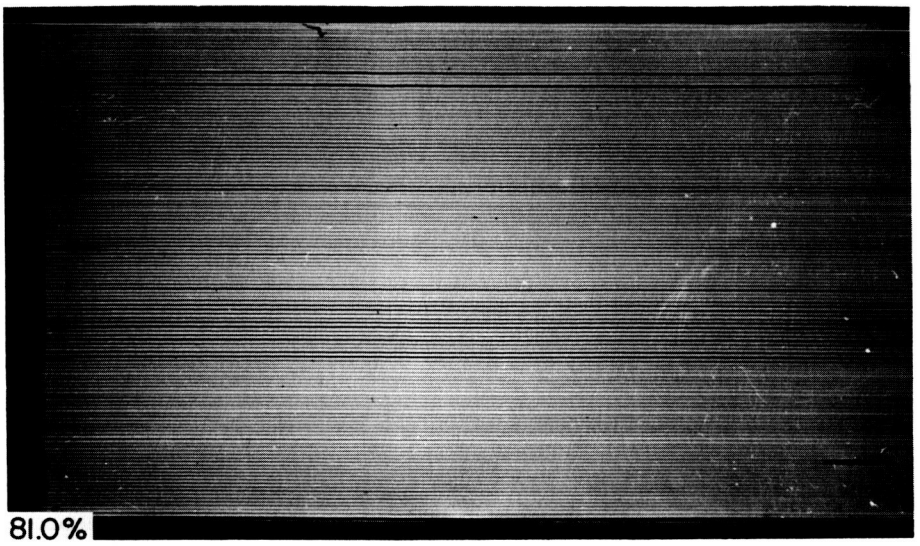

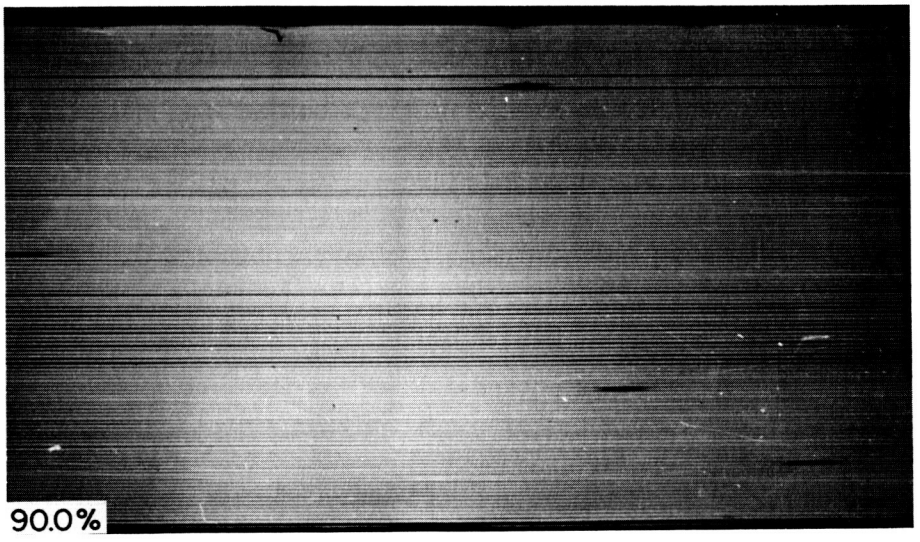

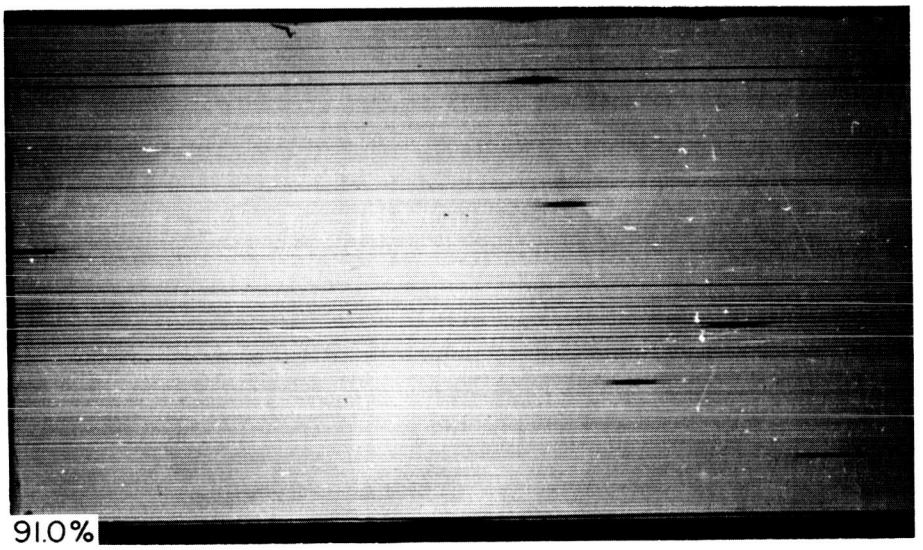

Figure 12 (Continued)

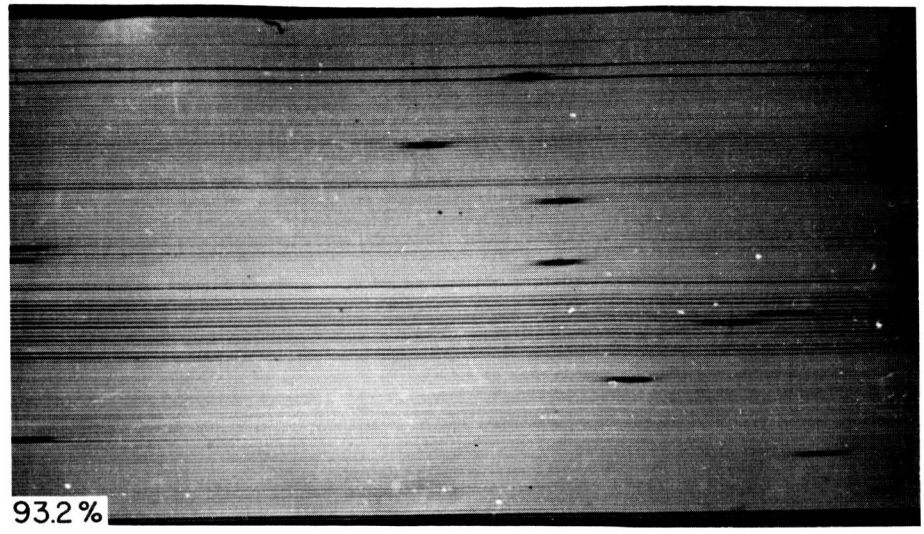

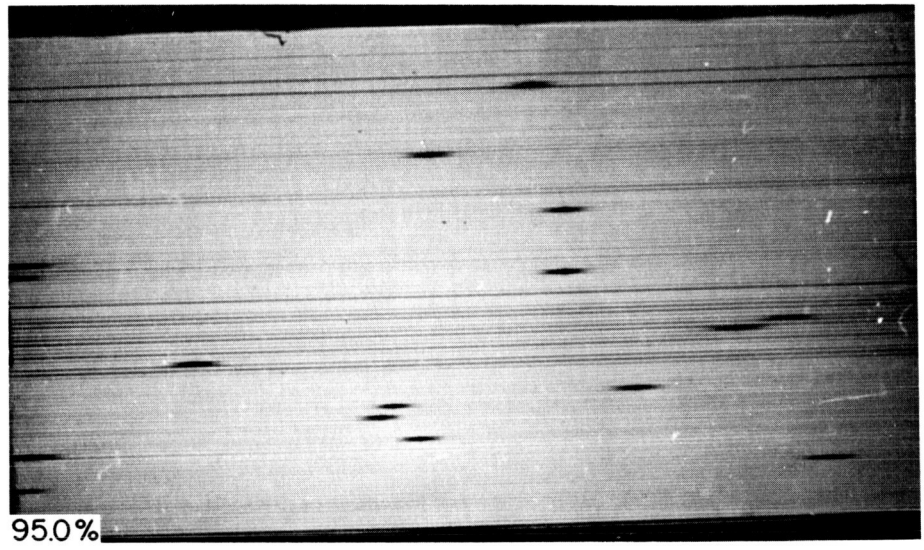

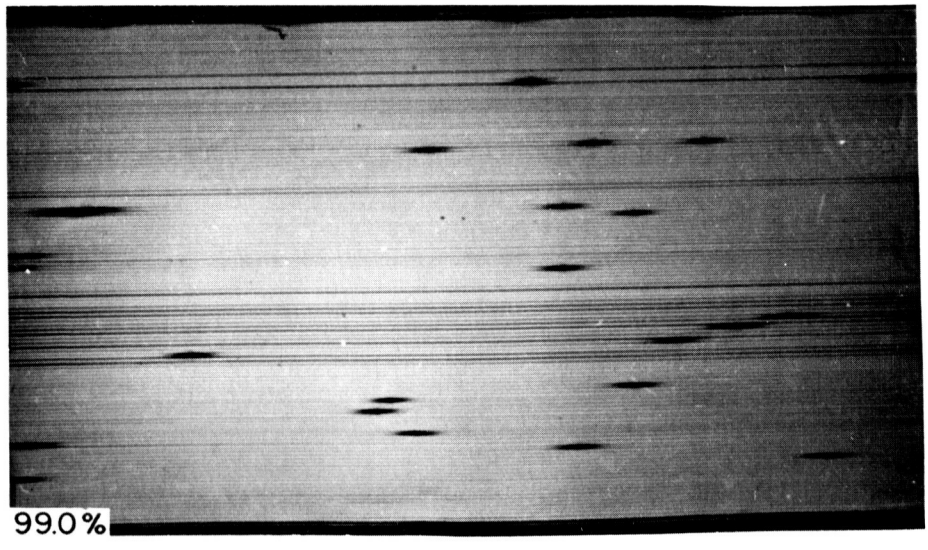

Figure 12 (Concluded)

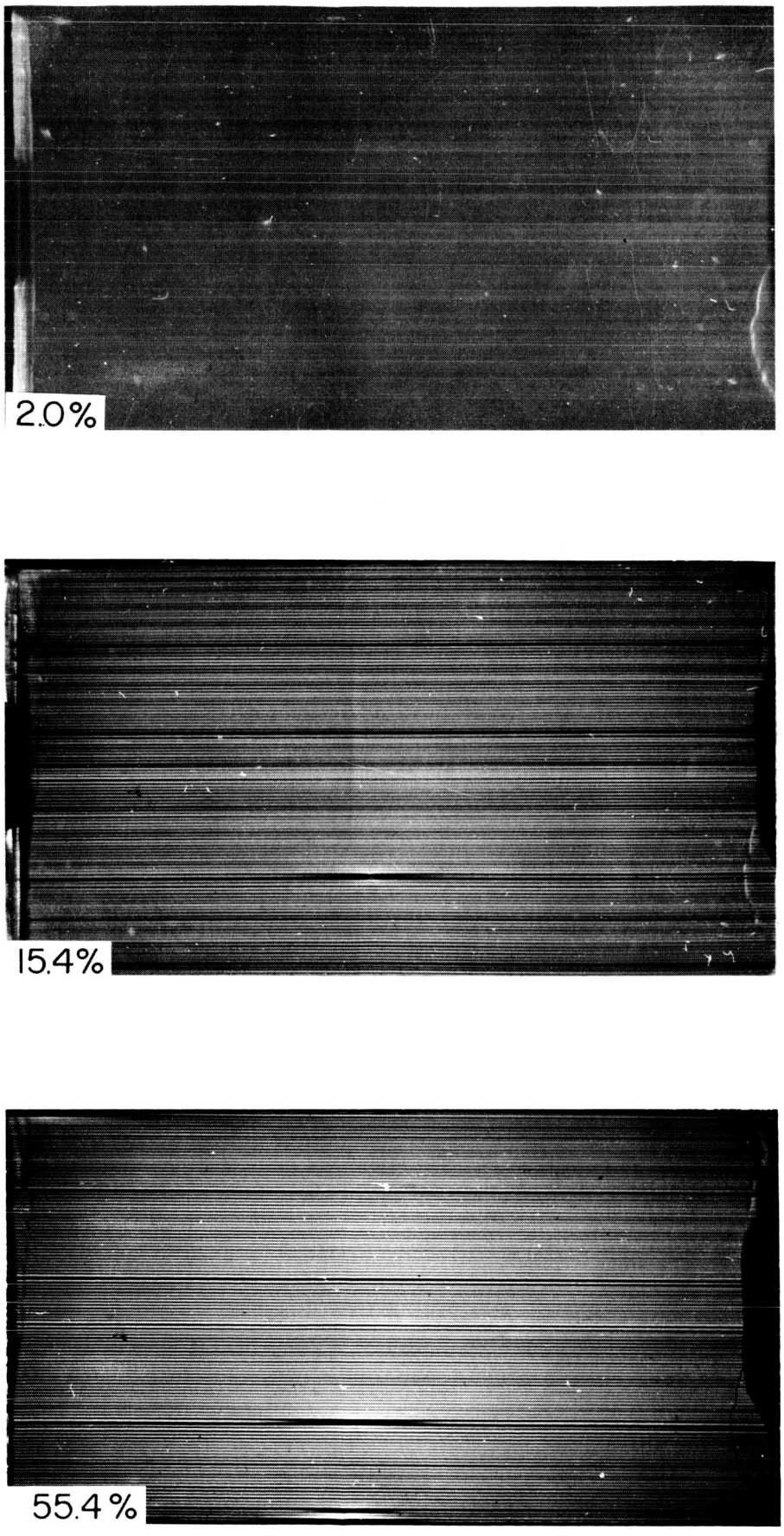

Figure 13. Failure Sequence of Specimen Having $E_b = 0.28$

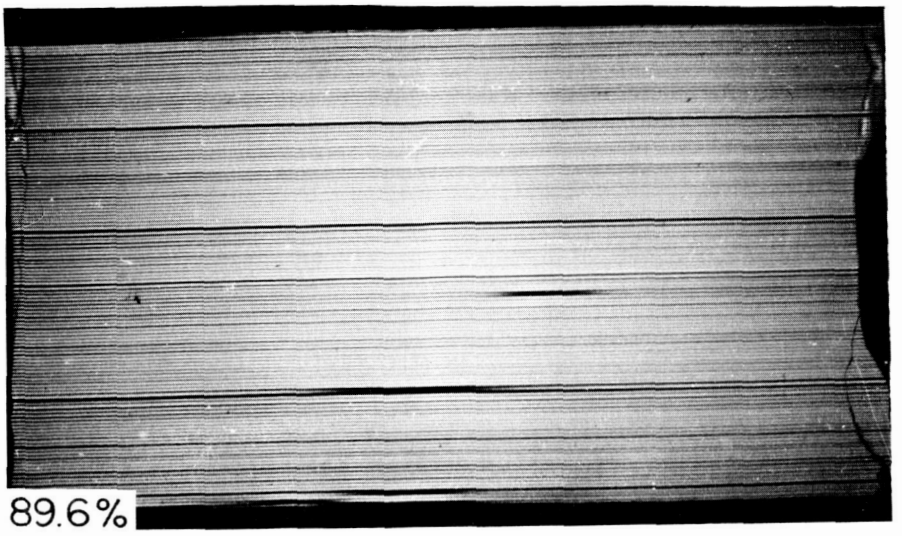

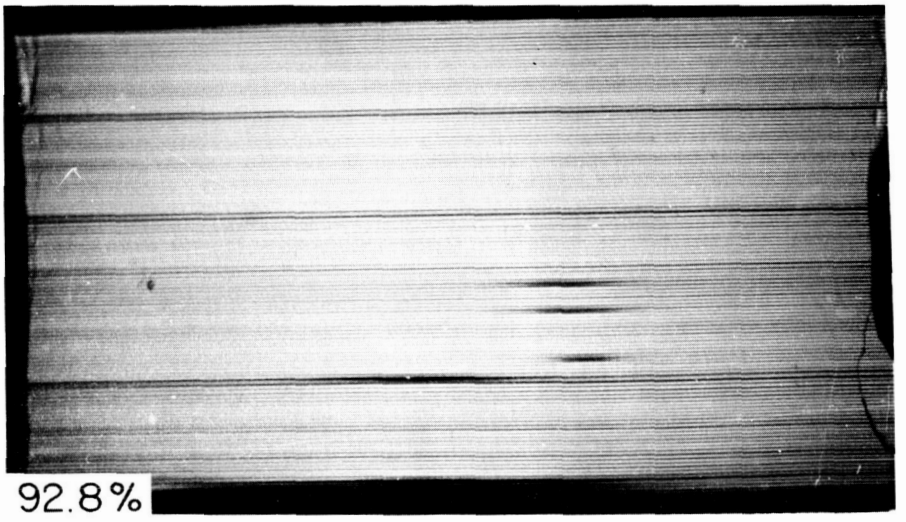

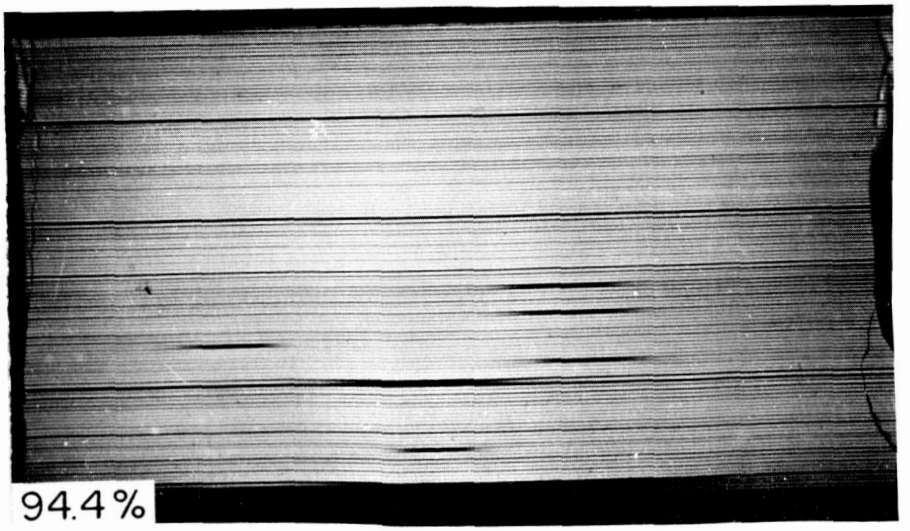

Figure 13 (Continued)

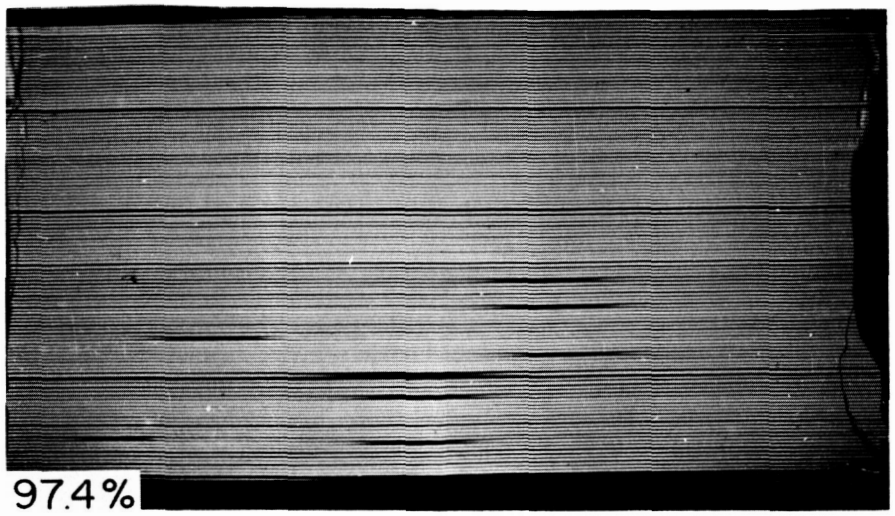

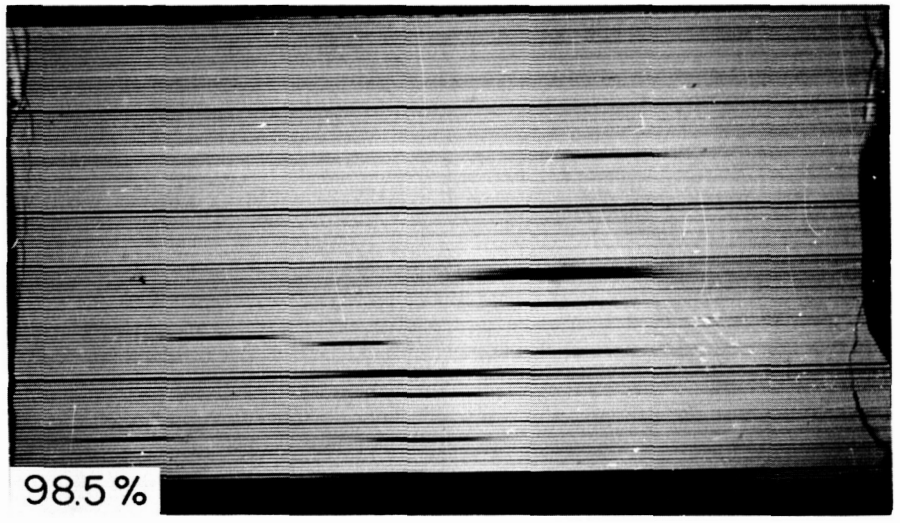

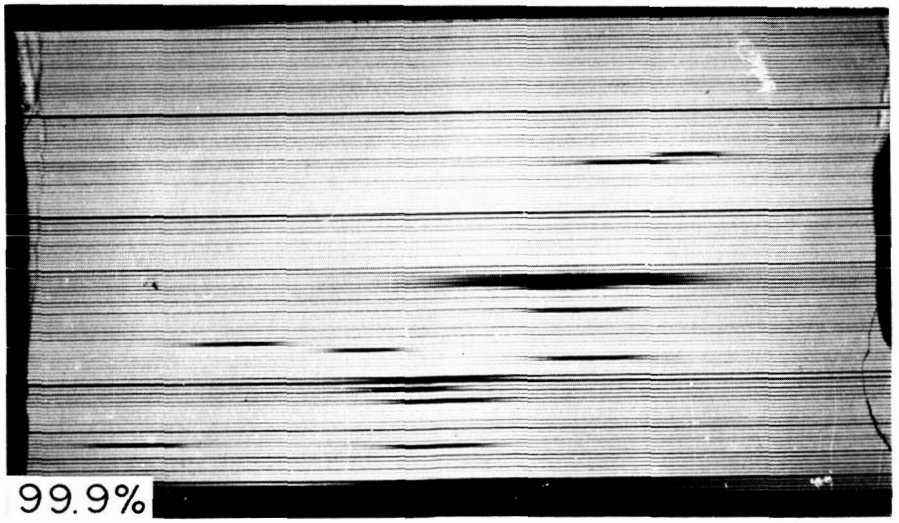

Figure 13 (Concluded)

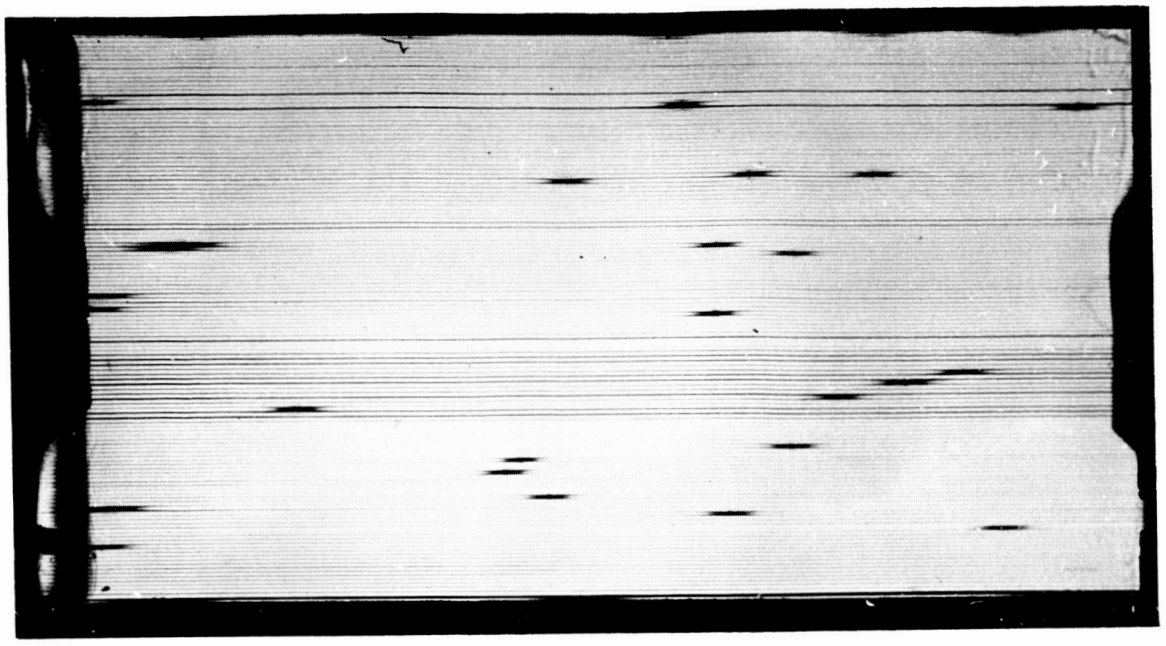

a. Matrix Modulus = 0.48×10^6 psi

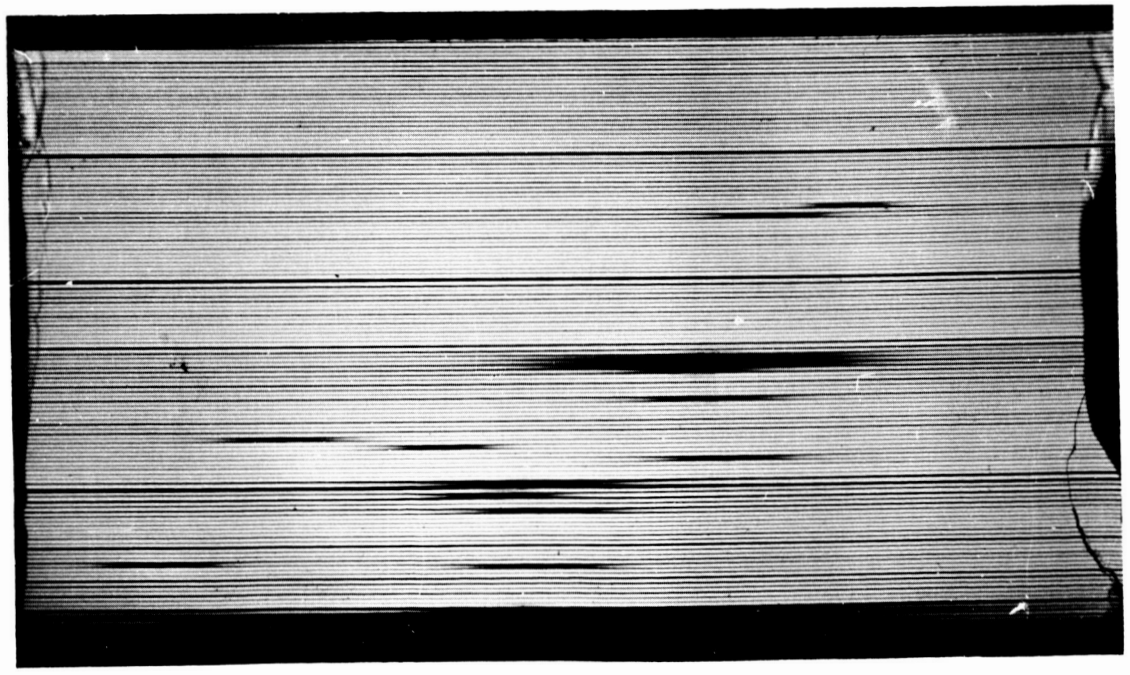

b. Matrix Modulus = 0.28×10^6 psi

Figure 14. Typical View of Tensile Failure Specimen of 99% of Ultimate Strength. Fibers are 0.0035" Diameter E-glass.

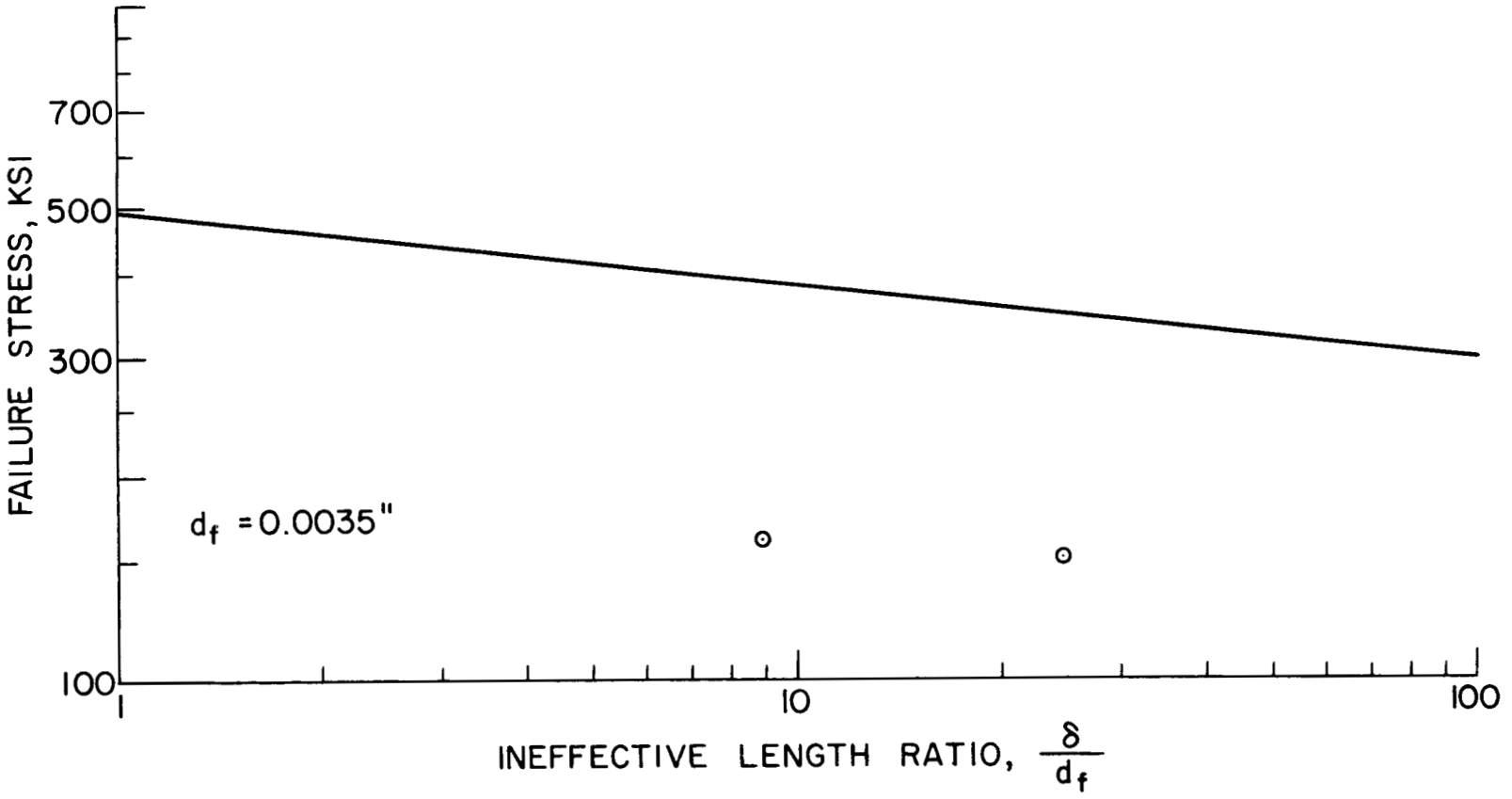

Figure 15. Composite Tensile Strength as a Function of the Fiber Ineffective Length.

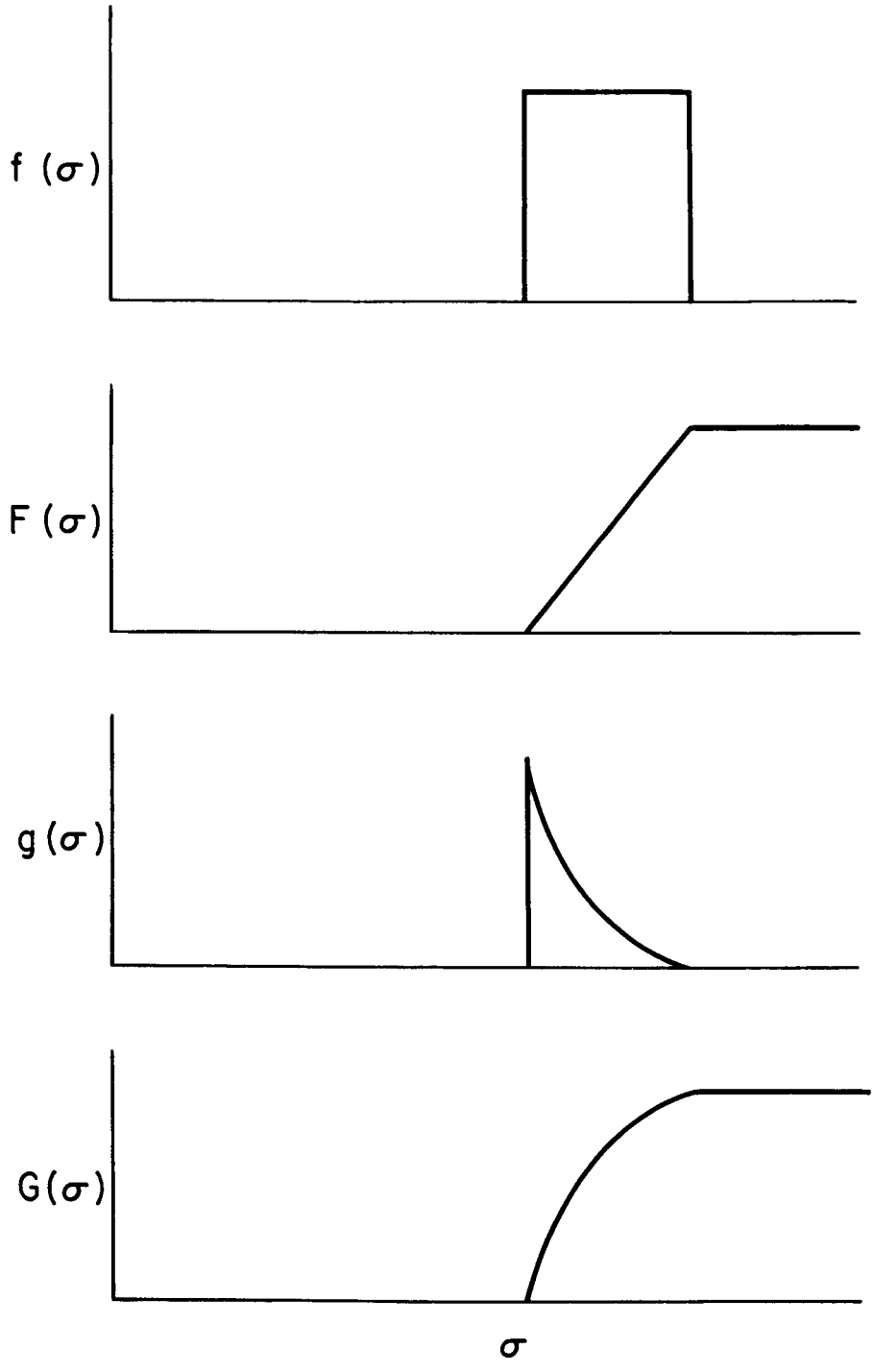

Figure 16. Rectangular Strength Distribution Function for the Links of a Chain.
a. Link Distribution Function
b. Link Cumulative Distribution Function
c. Chain or Fiber Distribution Function
d. Chain or Fiber Cumulative Distribution Function.

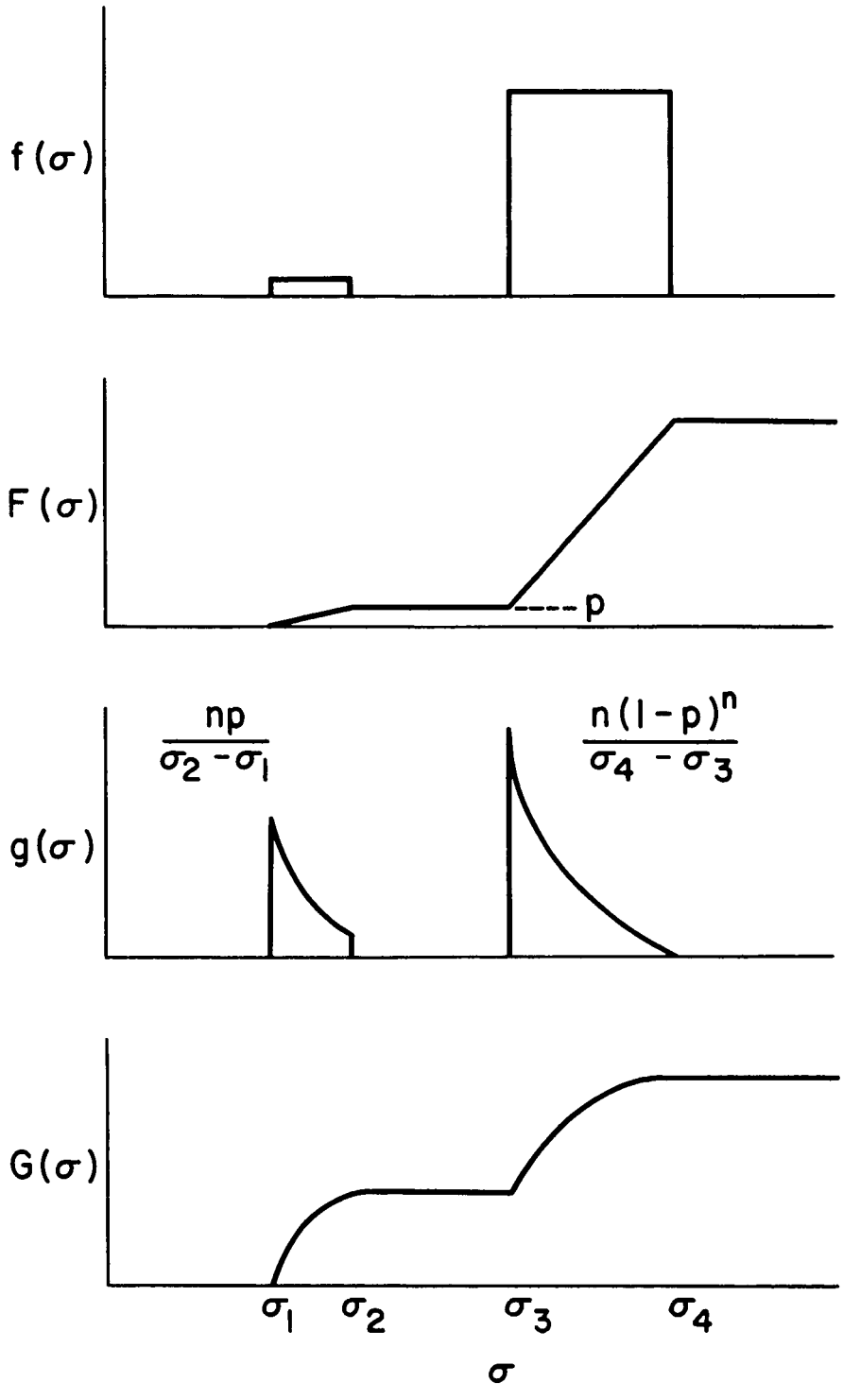

Figure 17. Double Rectangular Strength Distribution Function for the Links of a Chain

a. Link Distribution Function
b. Link Cumulative Distribution Function
c. Chain or Fiber Distribution Function
d. Chain or Fiber Cumulative Distribution Function.

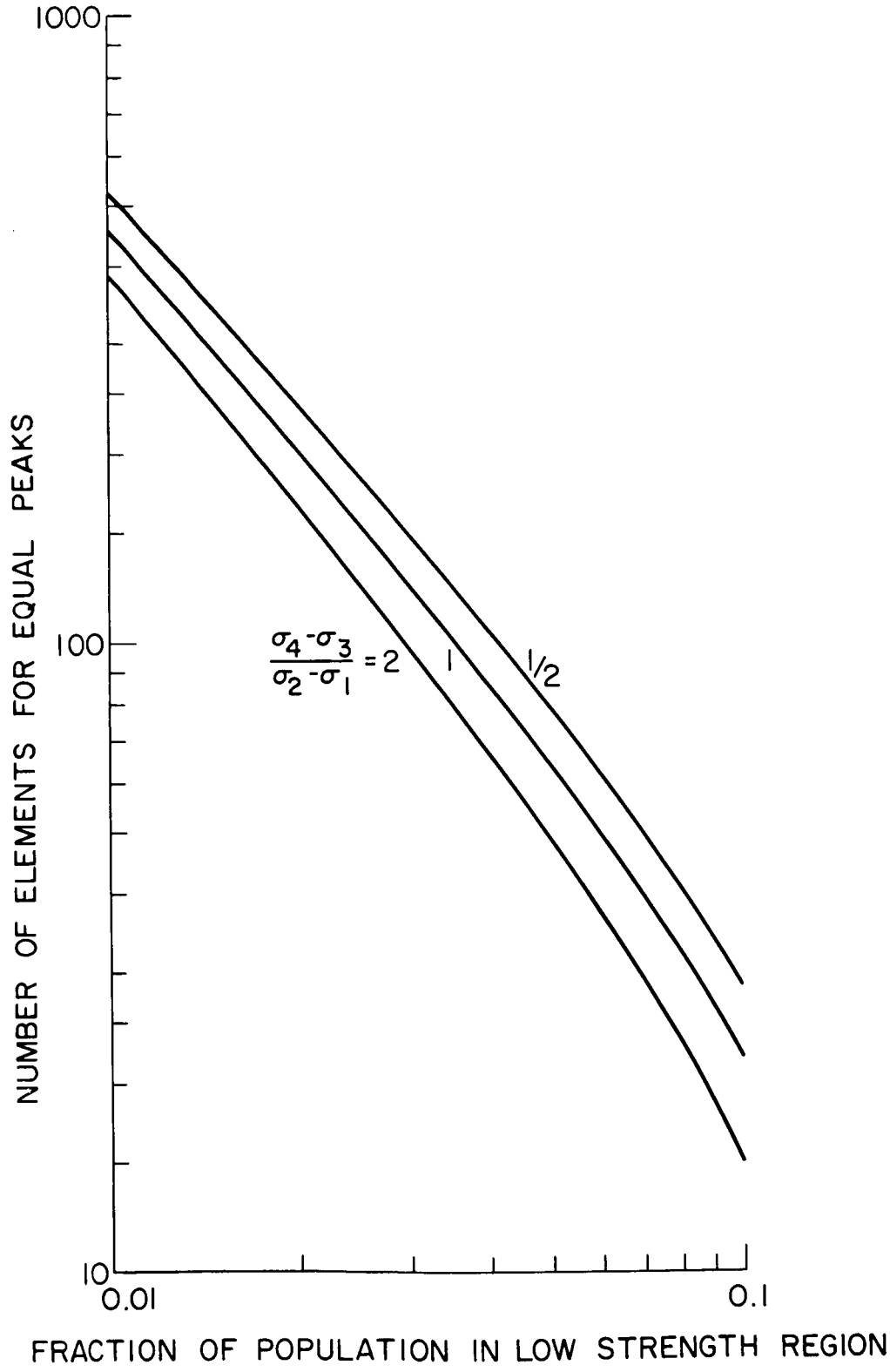

Figure 18. Number of Links in the Chain to Equate the Peaks of the Distribution Function Shown in Figure 15.

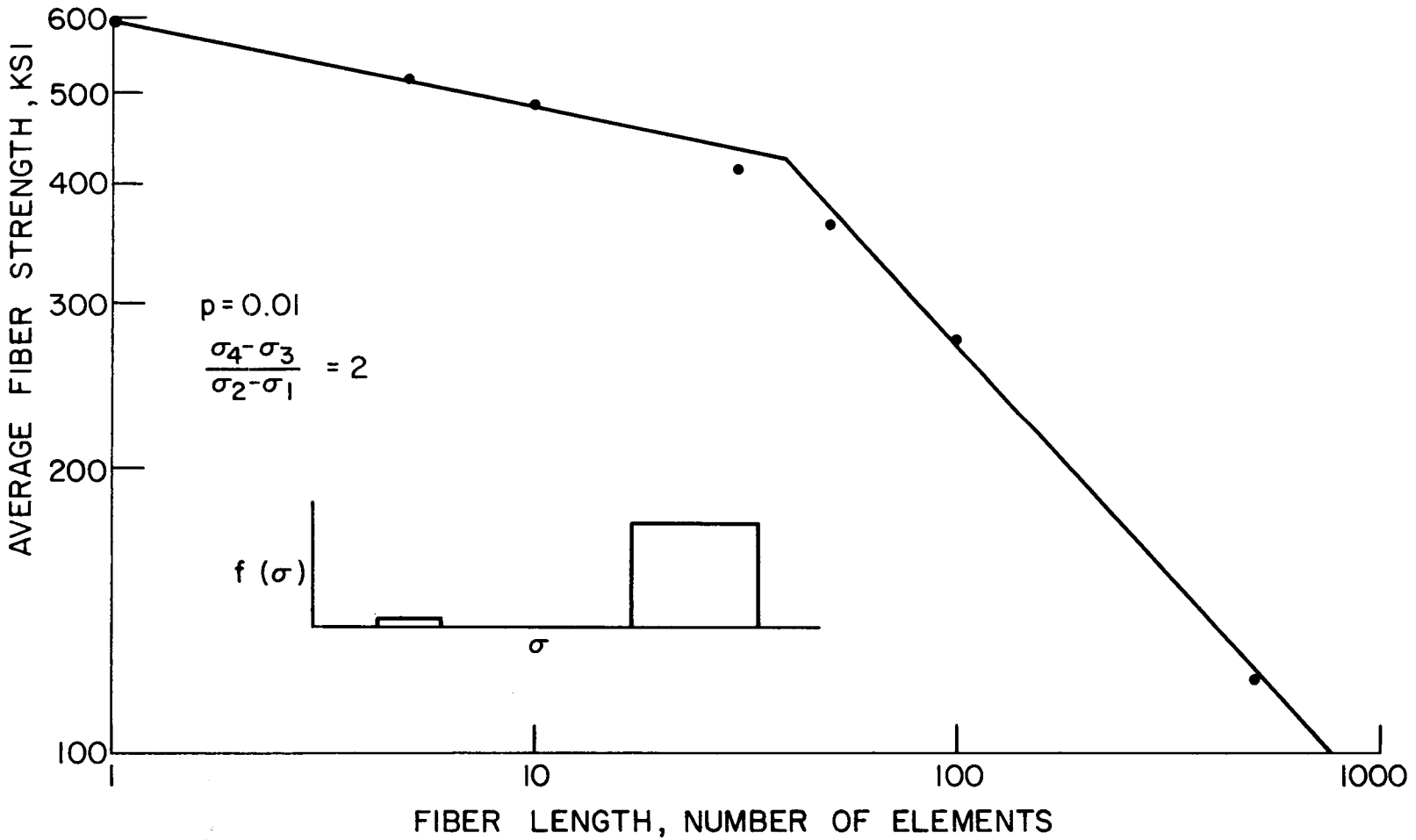

Figure 19. Mean Fiber Strength as a Function of Length for Fiber Links Having a Double Rectangular Strength Distribution Function.

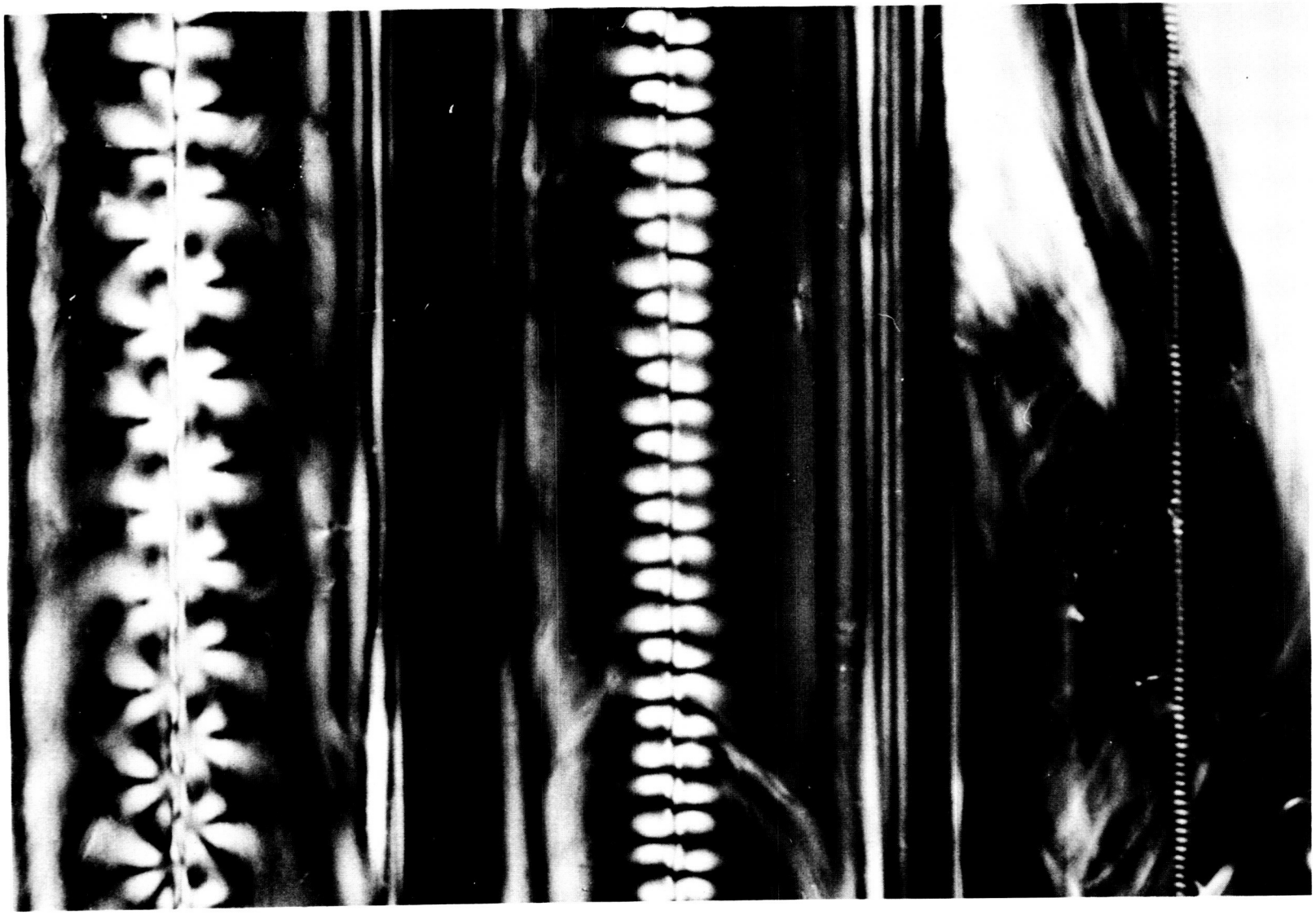

Figure 20. Photoelastic Stress Pattern for Three Individual E-Glass Fibers Imbedded in an Epoxy Matrix Showing Small Wavelength Buckle Patterns.

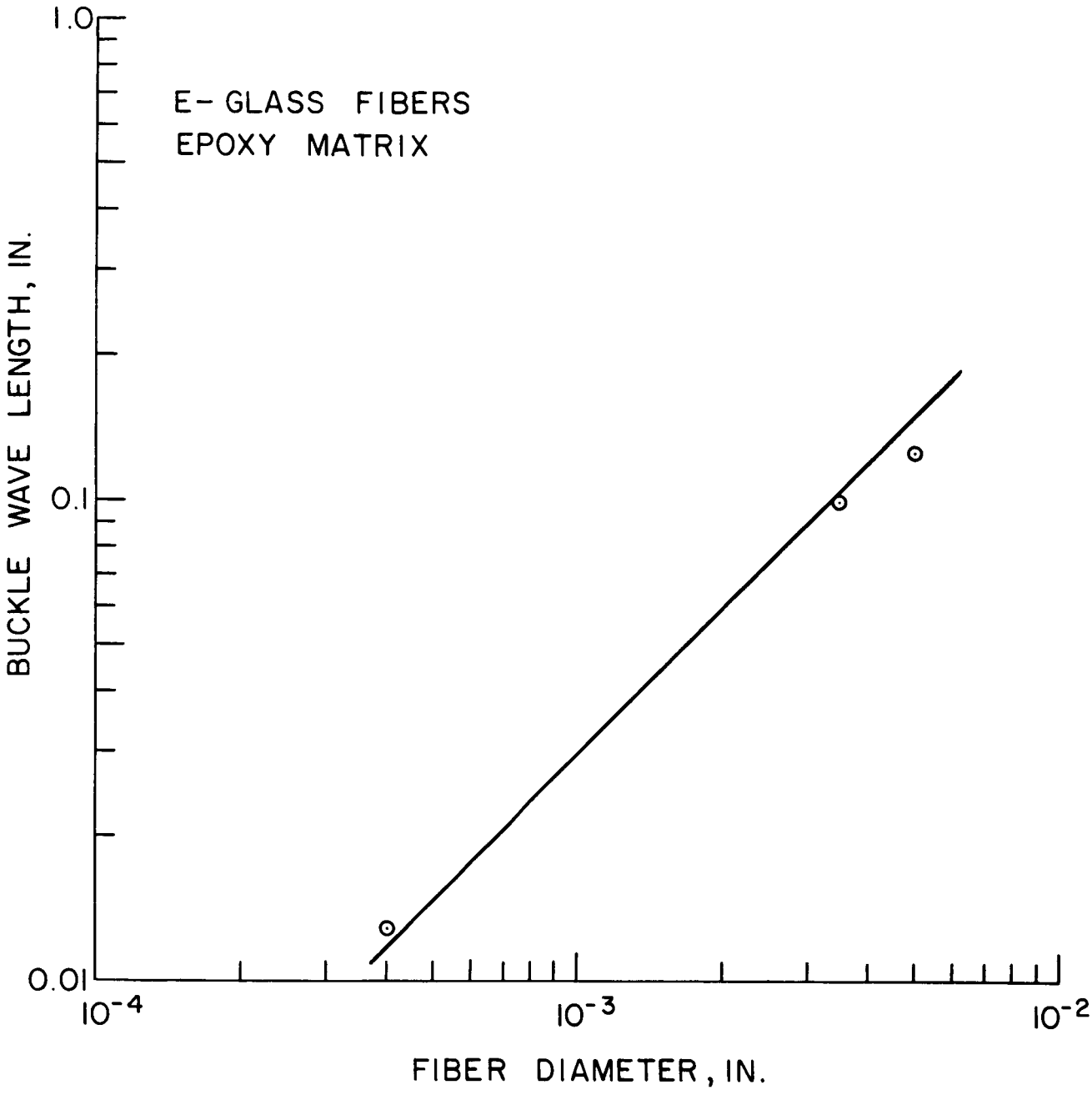

Figure 21. Experimental Results for Fiber Buckling Wavelength as a Function of Fiber Diameter.

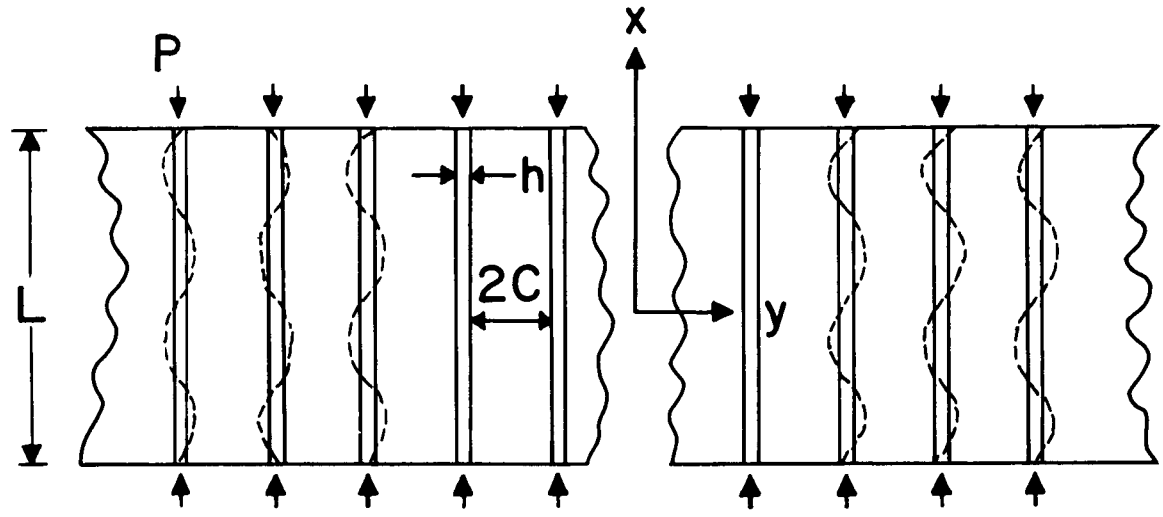

$$\Delta V_f + \Delta V_b - \Delta T = 0$$

$$P = \sigma_f h$$

$$V = \sum_n a_n \sin \frac{n\pi x}{L}$$

Figure 22. Analytical Model for Compressive Strength of Fibrous Composite.

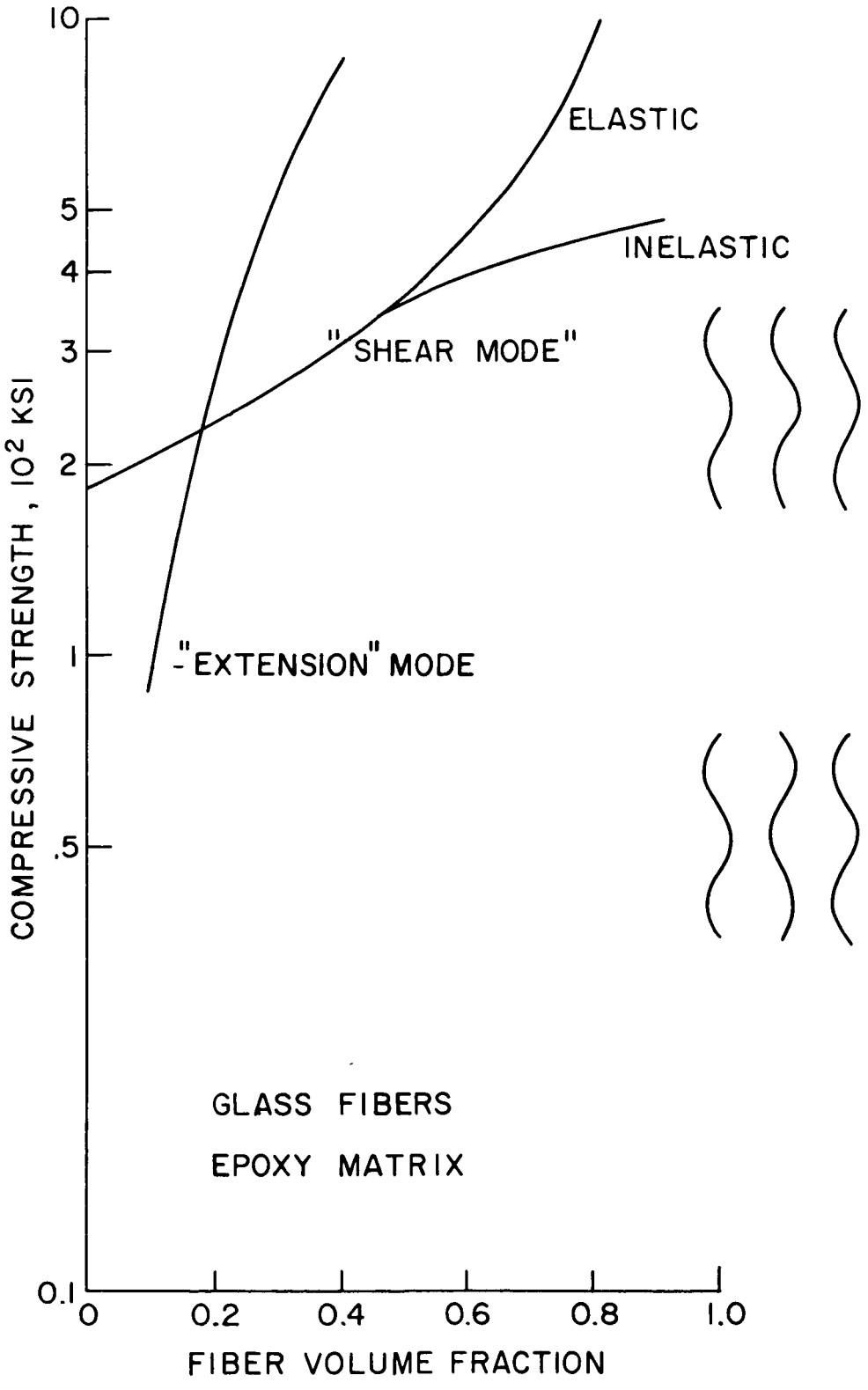

Figure 23. Compressive Strength of Glass Reinforced Epoxy Composites.

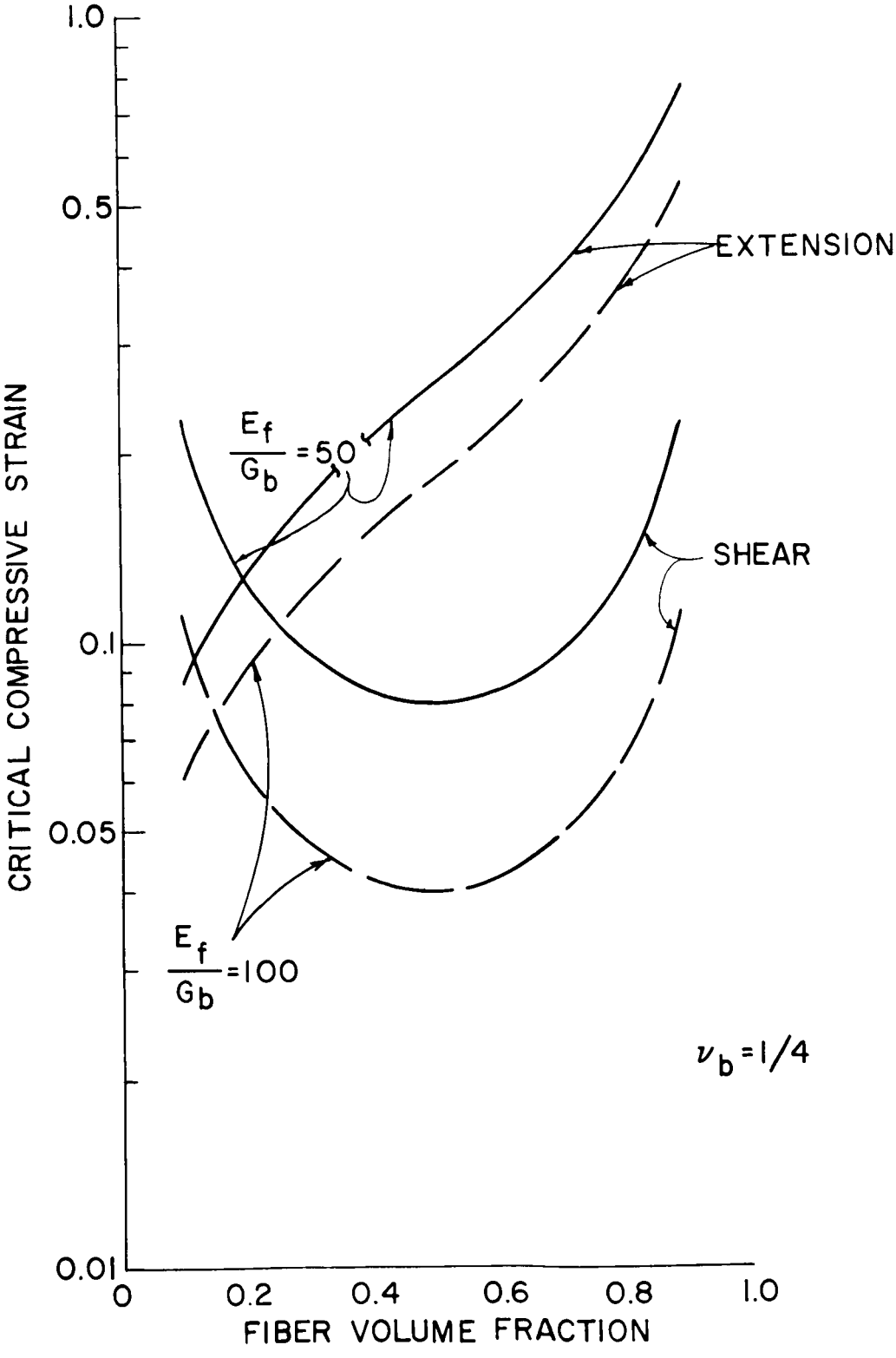

Figure 24. Critical Compressive Strain for Fibrous Composites.

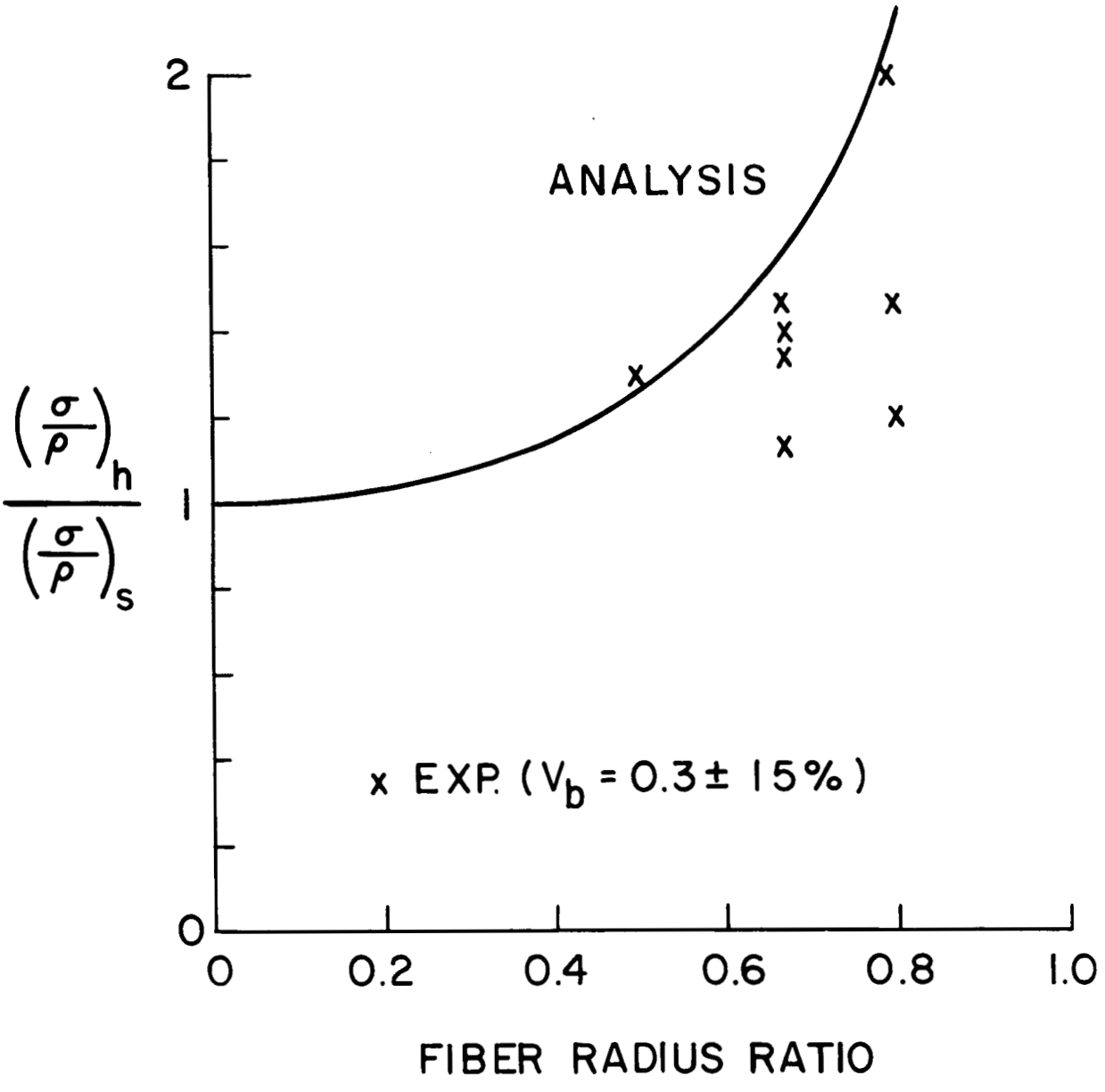

Figure 25. Comparison of Theory and Experiment for Compressive Strength to Density Ratio of Hollow Glass Fiber Composites.

GENERAL ELECTRIC

SPACE SCIENCES LABORATORY
MISSILE AND SPACE DIVISION

TECHNICAL INFORMATION SERIES

AUTHOR	SUBJECT CLASSIFICATION	NO.
B. W. Rosen	SPACE MECHANICS	R64SD80
		DATE: Nov. 1964
TITLE: MECHANICS OF COMPOSITE STRENGTHENING		G. E. CLASS: I
		GOV. CLASS: None
REPRODUCIBLE COPY FILED AT MSD LIBRARY, DOCUMENTS LIBRARY UNIT, VALLEY FORGE SPACE TECHNOLOGY CENTER, KING OF PRUSSIA, PA.		NO. PAGES: 72

SUMMARY

The development of very high strength and stiffness filaments has motivated considerable interest in the strength of fiber reinforced composites. This paper describes studies of the effect of fiber and matrix characteristics upon the mechanics of deformation and fracture of fibrous composites. These studies consider the response of a matrix reinforced by uniaxially oriented fibers. The strength of such a material is treated for the cases where the failure criteria are maximum tensile of compressive load carried by the composite in a direction parallel to the fiber orientation. Analytical models for failure in these two modes are developed. Comparison is made with available experimental data. The tensile failure model is a statistical one. A new experimental technique to investigate the validity of this model is described. All of the studies included attempt to relate composite performance to constituent properties.

KEY WORDS

Composite materials, filaments, deformation, fracture

BY CUTTING OUT THIS RECTANGLE AND FOLDING ON THE CENTER LINE, THE ABOVE INFORMATION CAN BE FITTED INTO A STANDARD CARD FILE.

AUTHOR B Walter Rosen

COUNTERSIGNED Norris F. Dow for FWN